Injectable hydrogel induces regeneration of naturally degenerate human intervertebral discs in a loaded organ culture model.

CHERIF, Hosni, LI, Li, SNUGGS, Joseph, LI, Xuan, SAMMON, Christopher <http://orcid.org/0000-0003-1714-1726>, LI, Jianyu, BECKMAN, Lorne, HAGLUND, Lisbet and LE MAITRE, Christine L. <http://orcid.org/0000-0003-4489-7107>

Acta Biomaterialia 176 (2024) 201–220

Contents lists available at ScienceDirect

Acta Biomaterialia

journal homepage: www.elsevier.com/locate/actbio

Full length article

Injectable hydrogel induces regeneration of naturally degenerate human intervertebral discs in a loaded organ culture model☆

Hosni Cherif[a], Li Li[a], Joseph Snuggs[b,c], Xuan Li[d], Christopher Sammon[e], Jianyu Li[a,d,f], Lorne Beckman[a], Lisbet Haglund[a,g], Christine. L. Le Maitre[b,c,*]

[a] Department of Surgery, McGill University, Montreal, QC H3G 1A4, Canada
[b] Oncology and Metabolism Department, Medical School, & INSIGNEO Institute, University of Sheffield, Sheffield, UK
[c] Biomolecular Sciences Research Centre, Sheffield Hallam University, Sheffield, UK
[d] Department of Mechanical Engineering, McGill University, Montreal, QC H3A 0C3, Canada
[e] Materials and Engineering Research Institute, Sheffield Hallam University, Sheffield, UK
[f] Department of Biomedical Engineering, McGill University, Montreal, QC H3A 2B4, Canada
[g] Shriners Hospital for Children, Montreal, QC H4A 0A9, Canada

ARTICLE INFO

Article history:
Received 2 October 2023
Revised 30 November 2023
Accepted 22 December 2023
Available online 30 December 2023

Keywords:
Injectable biomaterial
Intervertebral disc
Human organ culture

ABSTRACT

Low back pain resulting from disc degeneration is a leading cause of disability worldwide. However, to date few therapies target the cause and fail to repair the intervertebral disc (IVD). This study investigates the ability of an injectable hydrogel (NPgel), to inhibit catabolic protein expression and promote matrix expression in human nucleus pulposus (NP) cells within a tissue explant culture model isolated from degenerate discs. Furthermore, the injection capacity of NPgel into naturally degenerate whole human discs, effects on mechanical function, and resistance to extrusion during loading were investigated. Finally, the induction of potential regenerative effects in a physiologically loaded human organ culture system was investigated following injection of NPgel with or without bone marrow progenitor cells. Injection of NPgel into naturally degenerate human IVDs increased disc height and Young's modulus, and was retained during extrusion testing. Injection into cadaveric discs followed by culture under physiological loading increased MRI signal intensity, restored natural biomechanical properties and showed evidence of increased anabolism and decreased catabolism with tissue integration observed. These results provide essential proof of concept data supporting the use of NPgel as an injectable therapy for disc regeneration.

Statement of significance

Low back pain resulting from disc degeneration is a leading cause of disability worldwide. However, to date few therapies target the cause and fail to repair the intervertebral disc. This study investigated the potential regenerative properties of an injectable hydrogel system (NPgel) within human tissue samples. To mimic the human in vivo conditions and the unique IVD niche, a dynamically loaded intact human disc culture system was utilised. NPgel improved the biomechanical properties, increased MRI intensity and decreased degree of degeneration. Furthermore, NPgel induced matrix production and decreased catabolic factors by the native cells of the disc. This manuscript provides evidence for the potential use of NPgel as a regenerative biomaterial for intervertebral disc degeneration.

1. Introduction

Low back pain (LBP) is the leading cause of disability worldwide, and it is projected that by 2050 > 800 million people will have LBP globally [1]. Yet current therapies mainly treat the symptoms and do not target the cause, with low evidence of effectiveness [2]. Intervertebral disc (IVD) degeneration has been implicated in around 40 % of all chronic LBP cases [3], with a stronger as-

☆ Data Availability: The raw/processed data required to reproduce these findings cannot be shared at this time as the data also forms part of an ongoing study, but will be made available prior to final publication.

* Corresponding author.
E-mail address: c.lemaitre@sheffield.ac.uk (Christine.L. Le Maitre).

https://doi.org/10.1016/j.actbio.2023.12.041
1742-7061/

sociation seen in those individuals 50 years and under [4]. IVD degeneration has a multifactorial aetiology, including interaction of genetics, environmental factors, mechanical loading history and lifestyle factors [5]. The IVD is composed of three main tissue regions: the central gelatinous nucleus pulposus (NP); the surrounding concentric fibrous lamella of the annulus fibrosus (AF); and the superior and inferior cartilaginous end plates (CEP), which connect to the boney end plates of the adjacent vertebral bodies. During disc degeneration, the cells of the disc decrease anabolism and increase catabolism [5]. Decreased synthesis of normal matrix, particularly aggrecan and collagen type II within the NP, and increased production of matrix-degrading enzymes including matrix metalloproteinases (MMPs) and ADAMTS (A disintegrin and metalloproteinase with thrombospondin motifs) [5–9] leading to degradation of the matrix and increased fibrosis within the central NP region, altering the biomechanical properties of the disc [10–16]. These processes reduce the swell- re-swell properties of the disc which are essential to aid in the support of nutritional supply and waste removal during normal daily loading [17–23]. These changes in matrix synthesis and degradative enzyme production are driven at least in part by the local production of the catabolic cytokine interleukin-1 (IL-1), which is produced by the native NP and AF cells and increases during disc degeneration [24,25]. In addition to driving the changes in matrix synthesis and degradation, this cytokine also drives the production of a plethora of cytokines and chemokines within the native disc cells [25–27], and the production of angiogenic factors (e.g., VEGF) and neurotrophic factors (e.g., NGF and substance P) [28]. The combination of reduced nerve inhibiting matrix, particularly aggrecan [29,30], and decreased nerve inhibiting factors such as semaphorins [31,32], together with the increased production of neurotrophic and angiogenic factors [28,33,34] leads to the ingrowth of blood vessels and nerves into the normally aneural and avascular IVD [35–37]. These nerve fibres particularly follow cracks and fissures within the degenerate disc and can penetrate deep into the NP tissue [35,36], which is thought to contribute to the pain experienced during IVD degeneration. Furthermore, the IVD is an essential biomechanical unit of the spine and loss of its normal mechanical function during disc degeneration leads to altered mechanical stability and impingement of local nerve roots [15,38,39], and facet joint degeneration [40,41].

Regeneration of the IVD is a topic of great interest and debate [42–49], with a particular focus on the central region of the IVD, the nucleus pulposus (NP). However, to successfully regenerate the IVD and tackle the associated LBP it is essential to restore the mechanical properties of the disc, restore matrix producing cells to refill cracks and fissures, and decrease the catabolic cascade of matrix degradation. While also reducing inflammatory cytokines, angiogenic factors and neurotrophic factors within the degenerate disc which are produced by native IVD cells. Only in combination will such a regenerative therapy hope to tackle back pain associated with the degenerated disc. To date, several approaches have been investigated including a range of potential regenerative cell sources [49], with a number of these progressing to early clinical trials [46]. Alternatively, cell free approaches such as biomaterial implantation have been investigated [44], however these have suffered to date from poor integration with the local tissues and often lead to extrusion [50–53]. Whilst materials which are overly stiff will lead to increased stress on the endplate and can lead to endplate subsidence [54,55]. Many biomaterial approaches require surgical implantation or large-bore needle insertion [44,53,56], which could lead to AF damage and subsequent acceleration of degeneration [57–59]. A key question that remains in the regeneration of the IVD is whether a new cell source is required to induce regeneration, or indeed if such a cell source survives following implantation [45,46,49].

We have previously reported a thermally responsive hydrogel (NPgel) [60,61], which remains liquid above body temperature due to the maintenance of pNIPAM chains within a globule conformation upon the laponite® surface as described extensively within Boyes et al. [60], within this unfolded coiled conformation the polymer chains are hypothesized to form water-polymer interactions via amide groups. Upon cooling the globular pNIPAM on the Laponite® surface transform into a coli conformation at the lower critical solution temperature (LCST) which is adjusted to 37 °C by the inclusion of 13 % DMAC. During the transformation into the coiled conformation the polymer chains extend into the aqueous phase forming numerous physical interactions and entanglements with neighbouring laponite®-pNIPAM particles resulting in the formation of a gel. The final gelled NPgel system then mimics the mechanical properties of native NP tissue [62] and, following injection into a bovine degradation model, restored mechanical properties immediately after injection [62], where it was seen to fill the fissures generated by enzyme degradation [62]. Furthermore, we have previously demonstrated that NPgel induces the differentiation of bone marrow derived mesenchymal progenitor cells (BMPCs) into NP-like cells without the need for growth factors [61]. NPgel can be easily injected into IVD tissues which has been demonstrated using a bovine explant culture model [62], and more recently in an *ex vivo* goat organ culture model [63], where BMPCs were also successfully delivered to the tissues [62,63]. NPgel was shown to integrate with local tissues and promote new matrix production including aggrecan and collagen type II [62,63]. Interestingly, using a goat organ culture model, where physiological loading was maintained for a 3-week culture period, NPgel alone without BMPCs was sufficient to induce the native cells of the disc to increase matrix production with increases in aggrecan and collagen type II immunopositivity [63]. Furthermore, NPgel injection inhibited catabolic factors, including matrix degrading enzyme production and cytokines within the loading culture model of degeneration [63]. Within discs injected with NPgel together with BMPCs an increase in cellularity was observed, and cells also expressed high levels of aggrecan and collagen type II [63]. Decreased catabolic factors were also observed, but such decreases were also seen with NPgel injection alone, limiting observation of the possible additional effects of BMPC injection [63]. However, within this model, goat discs were subjected to enzyme digestion and load-induced degeneration over a short 1-week period, and thus these cells may show a higher regenerative capacity than naturally degenerate human discs [63]. Clearly, it is essential to investigate whether NPgel alone can induce a regenerative effect within naturally degenerate human IVD or whether the addition of a regenerative stem cell source is needed to induce regenerative effects.

Human IVD tissue can be obtained via two main routes for *ex vivo* investigations, firstly through surgical procedures, for example during discectomy surgery for nerve root compression. However, here the tissue obtained is fragments of tissue and thus *ex vivo* culture is limited to explant culture studies, such as constrained tissue explant cultures which can maintain normal tissue phenotype and structure during culture [64,65]. However, to obtain whole IVDs for investigation, cadaveric IVDs are required [66]. Such whole IVDs can be utilised within organ culture systems [66], where physiological loading can also be introduced to more closely mimic the natural in vivo loading and nutritional environment and investigate the potential of regenerative approaches [66]. Human organ culture systems have been developed which can maintain the viability of human IVDs for up to 4 months, under static conditions where the boney endplate is removed, but the cartilaginous endplate is retained prior to culture [67,68]. This has been successfully applied to investigate the potential of senotherapeutics within the IVD [68] under static culture conditions. The application of physiological loading to these cultures enabled the maintenance under

physiological conditions and retained viability of native and additionally injected NP cells delivered via a hyaluronan gel previously [69]. Moreover, in human IVDs with intact cartilaginous endplates cultured under simulated physiologic loads, NP and AF cells remained viable (~80 %) for the entire culture period of 14 and 21 days [70]. However, to date no such human organ culture system has been completed under physiological load where the boney end plates are retained; this would enable a closer mimic of the nutritional supply to the IVD, as the majority of the nutrients are delivered via diffusion through the cartilaginous and boney-endplates [18]. Thus such a system would be useful to assess the viability of such an approach within the large avascular human IVD [66].

Therefore, this study aimed to investigate several key questions essential to support translation to the clinic using human IVD tissues. Initially within an explant culture system the efficacy of NPgel, alone or in combination with BMPCs, to inhibit catabolism and promote anabolism was investigated. Whole human IVDs were further deployed to investigate injection capabilities of NPgel, and its effects on disc height and biomechanical properties including Young's modulus, failure strength and extrusion during failure. Finally, naturally degenerate whole human IVDs with an intact boney end plate were investigated over the course of 4-week culture to determine the ability of NPgel with or without BMPCs to promote anabolism, inhibit catabolism and restore mechanical properties, as a potential regenerative strategy for the IVD.

2. Methods

2.1. Experimental design

This study utilised human IVD tissues from two sources, NP tissue fragments from surgery and whole cadaveric IVDs, to investigate several phases of research to address key translational questions (Supplementary Figure 1). Firstly, the efficacy of NPgel with or without delivered BMPCs to inhibit catabolic and promote anabolic responses within degenerate human IVDs *ex vivo*, was investigated using NP tissue explants from NP tissue isolated during surgery for nerve root compression resulting from disc bulging. Tissue explants were cultured in a semi-constrained culture system which maintains tissue integrity and phenotype, preventing tissue swelling [65]. Tissue explants from matched patient samples were randomly assigned to non-injection control groups, or injection with either NPgel alone or NPgel + BMPCs. Explants were cultured for 6 weeks under 5 % O_2, 5 % CO_2 and following culture fixed, embedded and histology and immunohistochemistry utilised to investigate effects on anabolic and catabolic factors. Secondly, the ability of NPgel to be injected into naturally degenerate whole human IVDs and visualised during injection using the incorporation of a radio-opaque substance, enabling assessment of whether NPgel injection would result in a bolus or was capable of filling cracks and fissures. Post-injection MRI was utilised to identify NPgel location in addition to fluoroscopic imaging during injection. Thirdly, the immediate effects of NPgel injection on disc height and mechanical properties were investigated under simulated walking loads. Fourthly, injected discs were subjected to failure testing to determine whether NPgel was extruded. Finally, whole, naturally degenerate human IVDs were prepared including a thin layer of bone and maintained under physiological load. Following initial validation of cell viability of whole organ cultures, discs were either left untreated, injected with 500 µl of NPgel alone or 500 µl NPgel containing 1 M BMPCs. MRI was undertaken post-injection but pre-culture. Following the initial MRI imaging, injected discs and controls were placed under static load (0.1 MPa) for 48 h to enable equilibration, followed by dynamic, compressive loading (sinusoidal 0.1 MPa −0.6 MPa at 0.1 Hz), for two periods of 2 h each. The dynamic compressive loading periods were interrupted by recovery periods of 6 h and 14 h respectively, maintaining a low-static 0.1 MPa load. This 24 h loading protocol (2 h dynamic, 6 h static, 2 h dynamic and 14 h static) mimics the physiological loading during a daily sedentary routine [69]. The loading scheme was repeated for 26 additional consecutive days, resulting in a total loading period of 28 days (2 days static pre-load + 26 days physiological dynamic loading). Changes in disc height and axial load data were sampled and quantified to determine in-line mechanical properties of disc height difference, stiffness, modulus, range of motion, dissipated energy and normalised creep. A further MRI scan was performed post culture, discs were then fixed, EDTA decalcified and embedded to paraffin wax. Sagittal sections were taken, and tissue assessed by histology and immunohistology to determine the potential influence on anabolic and catabolic factors.

Table 1
Patient details for donated bone marrow used for extraction of bone marrow progenitor cells (BMPC) utilised within tissue explant studies.

Patient no.	Patient ID	Sex	Age	Sample Type	Pathology
1	P294	Male	67	Femoral head	OA
2	P299	Female	70	Femoral head	OA
3	P497	Female	72	Femoral head	OA
4	P498	Female	71	Femoral head	OA
5	P512	Female	57	Femoral head	OA

2.2. NPgel formulation

As previously published [61], an exfoliated suspension of 0.1 g Laponite® clay nanoparticles (25–30 nm diameter, <1 nm thickness) (BYK Additives Ltd, Cheshire, UK) was prepared in 10 mL ultra-pure water. 0.773 g N-isopropylacrylamide 99 % (NIPAM) (Sigma, Gillingham, UK), 0.117 g N, N' -dimethylacrylamide (DMAc) (Sigma, Gillingham, UK) and 0.01 g 2–2′-azobisisobutyronitrile (AIBN) (Sigma, Gillingham, UK) were added to the exfoliated Laponite® suspension, mixed and filtered using 5–8 µm pore filter paper. The suspension was polymerised at 80 °C for 24 h, stored at 60 °C, and cooled to 38 - 40 °C prior to the addition of cells or injection into tissue.

2.3. Bone marrow progenitor cell isolation and culture for human IVD explant studies

Human femoral heads from 5 individuals (Table 1), following hip replacement surgery for the treatment of osteoarthritis [Samples sourced with ethical approval from South Yorkshire and North Derbyshire Musculoskeletal Biobank (REC approval 15/SC/0132, HTA licence 12,182)], and were collected from Royal Hallamshire Hospital, Sheffield, UK with full patient consent. Bone marrow was extracted by mechanical force using a tissue biopsy punch, and washed in cell culture media. Bone marrow aspirate was filtered using a 100 µm cell strainer before being layered onto an equal amount of Histopaque®−1077 (Sigma) and centrifuged at 400 g for 30 mins at room temperature. Mononuclear cells within the opaque Histopaque-media interface were taken. The cells were washed in media and centrifuged at 400 g for 5 mins, this process was repeated twice. The cell pellet was finally resuspended in cell culture media and cultured in T75 tissue culture flasks (Nunc) at 37 °C with 5 % (v/v) CO_2 in a humidified environment, where the BMPC population adhered to the tissue culture plastic surface, BMPCs were utilised within tissue explant culture studies at passage 4 or less.

Table 2
Sample details for samples used within NP tissue explant study, Tissue was graded for degree of degeneration using NP features only as reported previously [71], within a scale of 0–9.

Patient no.	Patient ID	Sex	Age	IVD level	Grade of degeneration
1	HD511	M	69	L4/5	6
2	HD523	F	74	L4/5	6
3	HD533	M	34	L5/S1	5
4	HD541	M	39	C4/5	4
5	HD547	M	69	C5/6	7
6	HD548	F	60	C5/6	8
7	HD560	M	51	L3/4	5

2.4. Human nucleus pulposus tissue explant isolation, NPgel injection and culture

Human NP tissue was obtained from 7 patients from Sheffield Teaching Hospitals following microdiscectomy surgery for the treatment of nerve root compression resulting from IVD herniation with informed consent (Sheffield Research Ethics Committee (09/H1308/70)) (Table 2). A sample of IVD tissue from each patient was taken, fresh fixed and paraffin-embedded for histological grading of degeneration as previously reported [71]. Explants of NP tissue (5 mm diameter) were isolated from samples and placed within plastic rings to semi-constrain and reduce swelling of the tissue during the culture period as reported previously [65]. Explants were injected with 50 µL NPgel, with or without incorporated patient derived BMPCs (Table 1) at a cell density of 4×10^6 cells/ml, and cultured in DMEM (Life Technologies, Cat. No. 10,569,010) supplemented with 10 % (v/v) heat-inactivated FCS, 100 U/ml penicillin, 100 µg/ml streptomycin, 10 µg/ml ascorbic acid (all Life Technologies) and 250 ng/ml amphotericin (Sigma), at 37 °C in a humidified environment containing 5 % (v/v) O_2 and 5 % (v/v) CO_2 for 6 weeks, with media changed three times per week. Non-injected explants served as controls. Following culture, explants were washed in PBS and fixed for 48 hrs in 10 % neutral buffered formalin (Leica Biosystems), and processed into paraffin wax, prior to downstream analysis.

2.5. Human cadaveric disc radiographic grading and selection

Human spinal segments from T9/T10 to L5/S1 were obtained after informed consent through the Transplant Quebec Organ Donation Program (Tissue Biobank 2019–4896). Lateral lumbar spine radiographs of each subject IVD levels available between T9–10 and L5/S1 were investigated and digitised. The quantitative assessment for the presence and severity of disc degeneration was based on Wilke's grading system [72]. Radiographic assessments were performed, and the grading system consists of three variables: "height loss", "osteophyte formation", and "endplate sclerosis", each graded on a scale from 0 to 3. The overall degree of degeneration for each IVD was then determined by summing the three scores and classified as follows: Grade 0 (score 0, no degeneration), Grade 1 (score 1–3, mild degeneration), Grade 2 (score 4–6, moderate degeneration) and Grade 3 (score 7–9, severe degeneration). Anterior and posterior disc heights and IVD depth were measured as previously reported [73]. Patient demographics and degeneration grade of each cadaveric disc utilised in this manuscript are provided in Table 3.

2.6. Human cadaveric disc isolation for injection testing and mechanical analysis

Human IVDs were isolated as described previously [67,69] from lumbar spine segments obtained after informed consent through the Transplant Quebec Organ Donation Program (IRB# A04-M53–08B) (Table 3). Discs for initial injection and mechanical analysis were isolated from frozen spines and prepared with intact vertebral bone, radiographs were captured from transverse and sagittal planes together with a scale to calculate accurate disc heights. Then, discs were pre-warmed to 37ºC prior to testing.

2.7. Injection testing, mechanical analysis and failure testing in cadaveric human discs

Radiographs were captured from transverse and sagittal planes together with a scale to calculate accurate disc heights. Discs were pre-warmed to 37ºC prior to mechanical analysis, discs were preloaded at 0.1 MPa for 30 s prior to 6 cycles at 0.53–0.65 MPa 1 Hz (simulated walking) which was repeated 3 times to calculate Young's Modulus during simulated walking. Following initial mechanical testing, discs were injected with pre-warmed NPgel (>37ºC) containing Iohexol using fluoroscopy through a 25-gauge needle to visualize injection until maximal filling pressure was felt. The total injection volume was recorded for each IVD. Following injection, radiographs were captured on transverse and sagittal planes. Following pre-warming to 37ºC for 30 mins post-injection, discs were firstly re-analyzed using simulated walking to determine modulus following injection. Finally, discs underwent ultimate strength testing by compression at a speed of 2 mm/min until failure. Video capture was utilized to determine whether any NPgel extruded. MRI measures were performed before loading for pre-injected IVDs and after loading post-injection.

2.8. Human cadaveric disc isolation for live organ culture studies

Human IVDs were isolated as described previously [69] from lumbar spine segments obtained after informed consent through the Transplant Quebec Organ Donation Program (IRB# A04-M53–08B) (Table 3). Within 4 h post-mortem, discs were radiographed and those with degeneration grades of 2 (moderate degeneration), (using the lumbar spine radiographic grading system of Wilke et al. [72]) were selected. Live discs were isolated by parallel cuts close to the endplates leaving approximately 0.5 mm bone on each side of the discs. The disc height was measured, then the bony-endplate thoroughly rinsed in PBS containing 200 µg/mL Primocin (InvivoGen, San Diego, CA, USA) and 1 µg/mL Amphotericin B (ThermoFisher Scientific, ON, CA), followed by 2 washes in Hanks' balanced salt solution (HBSS, Sigma) also containing 200 µg/mL Primocin (InvivoGen, San Diego, CA, USA) and 1 µg/mL Amphotericin B (ThermoFisher Scientific, ON, CA to ensure all blood clots were removed and processes were clear. Washed discs were then placed in sterile polypropylene specimen containers (80 mL volume, STARPLEX Scientific, Etobicoke, ON) containing culture media (Dulbecco's Modified Eagle's Medium, #D5030 and #D1152, Sigma, ON, CA) supplemented with 2 mM GlutaMAX™, 5 % foetal bovine serum (ThermoFisher Scientific, ON, CA), 100 μg/mL Primocin (cat. Code: ant-pm-2, InvivoGen, San Diego, CA, USA), and 50 μg/mL ascorbic acid (#A4403, Sigma, ON, CA) at a ratio of 3.5 mL of media per gram of tissue weight [68,74]. Discs were maintained in culture media to equilibrate for about 16 h and were then prepared for autologous injections and MRI scans.

2.9. Metabolic activity

An initial pilot study was performed to ensure the viability of the organ cultures as prior validations have been completed on whole discs without bone in the bioreactor system [67–69]. Thus, an initial pilot viability study was performed on non-injected discs to evaluate metabolic cell activity following culture by Alamar blue assay. Sixteen discs from 4 donors (Table 3) were cul-

Table 3
Donor demographics for cadaveric discs, and studies utilised for. Grade of degeneration determined radiographically and scored on a scale of 0–3 [72].

Donor id.	Sex	Age	IVD level	Grade of degeneration	Study component
1	M	44	L1/2	1	Injection testing and Mechanical Analysis
	M	44	L2/3	1	
	M	44	L3/4	2	
2	M	52	T12/L1	1	Injection testing and Mechanical Analysis
	M	52	L1/2	1	
	M	52	L2/3	1	
	M	52	L3/4	1	
	M	52	L4/5	1	
3	M	69	L4/5	1	Injection testing and Mechanical Analysis
	M	69	T9/10	1	
4	F	38	T9/10	1	Viability testing – organ culture
	F	38	L2/3	1	
	F	38	L3/4	2	
	F	38	L4/5	2	
5	F	45	L1/2	1	Viability testing – organ culture
	F	45	L2/3	1	
	F	45	L3/4	2	
	F	45	L4/5	2	
6	M	47	L1/2	2	Viability testing – organ culture
	M	47	L2/3	1	
	M	47	L3/4	1	
	M	47	L4/5	2	
7	M	68	L1/2	2	Viability testing – organ culture
	M	68	L2/3	1	
	M	68	L3/4	1	
	M	68	L4/5	2	
8	F	45	L3/4	2	Organ culture – None-injected
9	F	68	L2/3	2	Organ culture – NPgel
			L4/5	2	Organ culture – NPgel +BMPCs
10	M	47	L1/2	2	Organ culture – NPgel +BMPCs
	M	47	L2/3	2	Organ culture – NPgel
11	M	78	L1/2	2	Organ culture – NPgel +BMPCs
12	F	78	L3/4	2	Organ culture – None-injected
13	F	53	L1/2	2	Organ culture – NPgel +BMPCs
	F	53	L2/3	2	Organ culture – NPgel
	F	53	L4/5	2	Organ culture – NPgel +BMPCs
14	F	69	L1/2	2	Organ culture – None-injected
	F	69	L2/3	2	Organ culture – NPgel
	F	69	L3/4	2	Organ culture – NPgel
15	M	54	L1/2	2	Organ culture – NPgel
			L2/3	2	Organ culture – None-injected
			L4/5	2	Organ culture – None-injected

tured under dynamic and static culture for a total of 28 days. Following 28 days of culture, 6 mm cores were taken from the NP and inner AF (iAF) regions, using a biopsy punch (Acuderm Inc., Ft. Lauderdale, FL). The tissue core was weighed then incubated in culture medium containing 10 % Alamar Blue® (Thermo Fisher, Waltham, MA, USA) and incubated for 6 h at 37 °C as reported previously to measure metabolic activity [75]. After exposure, Fluorescence (Ex560/Em590) was measured by using a spectrophotometer (Tecan Infinite T200, Männedorf, Switzerland) equipped with Magellan software (Tecan, Männedorf, Switzerland). Results are presented as an average fluorescence intensity per gram of tissue. Experiments were performed in triplicates.

2.10. Injection of hydrogel and hBMPCs cell-suspension

NPgel was injected into native disc tissue with a 25 G needle (REFs). To evaluate the feasibility of tissue repair strategies with cell supplementation, human bone marrow mesenchymal progenitor cells (hBM-MSCs, RoosterBio, Inc. Cat. #MSC-001, Lot.#00,136 (20 yr-old female)) (BMPCs) (Utilised at passage 1, which had been expanded in low (2.25 g/L) glucose DMEM supplemented with 10 % FBS, 5 ng/mL fibroblast growth factor 2, 2 mM GlutaMAXTM, 50 µg/mL Gentamicin (ThermoFisher Scientific, ON, CA)), suspended (1 million /500uL) in NPgel as described previously. The NPgel and BMPCs seeded in NPgel injection therapy was studied using the bioreactor system and 16 human IVDs cultured *ex vivo*.. Discs were injected with either $\sim$ 500 μL of NPgel or $\sim$ 500 μL of NPgel seeded with 1 $\times$ 10^6 hBMPCs, non-injected discs served as controls (Table 3). The hydrogel was injected laterally into the central NP region using a 25-Gague needle. Injected discs underwent MRI immediately following injection. They were then placed under static load (0.1 MPa) for 48 h and then dynamically loaded as described below for 26 additional days. After loading was completed, post-culture MRI scans were performed, and tissue was fixed and processed for histopathological examination.

2.11. Magnetic resonance imaging and analysis

T1ρ-weighted MRI directly correlates with proteoglycan content in IVDs of intact human lumbar spine segments [69]. To determine the effect of cell/gel therapy on degenerate intact human lumbar discs, potential region of interest (ROI) in NP and AF areas were identified as previously described [68] and the average of the T1ρ values calculated within the ROIs of the control and injected discs slices per image. Briefly, discs were sutured on one side (to mark for MRI positioning) and were allowed to equilibrate for 24 h in culture media pre-injection. They were subjected to pre-T1ρ MRI scans and then cultured under dynamic loading for 28 days. Post-

culture and after 24 h equilibration period, post-T1ρ MRI scans were acquired. All isolated human discs were scanned in sagittal and axial planes and images were obtained on a 7T Bruker BioSpec 70/30 USR (Bruker Biospin, Milton, ON, Canada) with the high-performance mini-imaging kit gradient upgrade AVIII electronics (Bruker) and a Bruker-issued T1ρ-RARE pulse sequence, as previously established [68,69]. Heat maps representing signal intensity were created using the MIPAV software (NIH Center for Information Technology, Bethesda, MD, USA). T1ρ values were calculated and quantified for all the axial slices using the MIPAV software. T1ρ values of 'before' and 'after' scans of each disc were normalized to the surrounding culture medium (strongest value) using editing features in MIPAV software. Specific regions of interest (ROIs) were drawn around regions indicating NP region of the 'after' images and superimposed onto the same region of the 'before' image. This was performed in the axial plane of slices 3–7 (out of 8) for each sample. The T1ρ images were manually cropped by a single user (DHR) around the perimeter of the IVDs. The average of the T1ρ values was calculated within the ROIs for the hydrogel alone and the cell-seeded hydrogels from 3 to 7 slices per image in the axial plane. After MRI analysis, discs were fixed in 16% w/v periodate lysine paraformaldehyde (PLP) in PBS fixative for 48 hrs prior to 10 % neutral Buffered formalin and EDTA decalcification, prior to histological processing.

2.12. Disc culture and loading regimes

The bioreactor system design and culture approach for human lumbar IVDs has previously been described [68,69]. Briefly, non-injected, NPgel and NPgel+BMPCs live discs were loaded statically for 48 h at 0.1 MPa allowing the discs to creep, thereby equilibrating their water content to the external load and intrinsic swelling properties. Dynamic, compressive loads were applied to the groups cycling in a sinusoidal pattern between 0.1 MPa and 0.6 MPa at 0.1 Hz for two periods of 2 h each. The dynamic compressive load periods were interrupted by recovery periods of 6 h and 14 h respectively, maintaining a low-static 0.1 MPa load. The loading scheme was repeated for 26 consecutive days and changes in disc height and axial load data were sampled continuously at 0.2 Hz. After loading was completed, discs were packed in a sterile bag filled with 25 mL of culture medium, sealed, and taken for post-treatment T1ρ MRI scans.

2.13. Biomechanical analysis

Changes in disc height and axial load data were sampled and quantified as previously described [68] using MATLAB software. For analysis of the biomechanical parameters of each cyclic dynamic and low-static loading, the daily loading data was divided into 4 segments, which were laid between 4 points of interest at 2 h (POI-1), 8 h (POI-2), 10 h (POI-3), and 24 h (POI-4) respectively. A MATLAB code was used to extract defined biomechanical parameters from the raw force-displacement data in cyclic loading or static loading corresponding to each point of interest as previously described [76,77]. Stiffness was defined as the slope of the force-displacement curve from the minimum to the maximum displacement region. Similarly, the modulus was determined as the slope of the stress-strain curve. Here, these two parameters are characterized as homogenized "effective" linear elastic stiffness and modulus of the entire disc. This type of measurement characterizes the average linearized behavior of the entire disc, treating it as a homogeneous elastic material. As previously reported [78], this characterization simplifies the more complex behavior of a real disc. However, it provides a single metric for quantifying the mechanical behavior of the entire disc and facilitates comparison of disc behavior among each loading day, various points of interest, and different experimental groups. Range of motion (ROM) was the total displacement of the motion segment during a compression cyclic load. Dissipated energy was defined as the area between loading and unloading curves in the force-displacement response in the cyclic load. The preceding parameters are determined from the average of 5 test cycles where the point of interest is located. In the low-static recovery periods (POI-1 to POI-2, POI-3 to POI-4), the creep strain at POI-2 or POI-4 along with time was normalized to the initial strain at POI-1 or POI-3 respectively. Specifically, strain (σ_{pt}) at a point is equal to the disc height change ($H_{initial}$-H_{pt}) divided by the initial disc height ($H_{initial}$), that is $\sigma_{pt}=(H_{initial}-H_{pt})/(H_{initial})$. The normalized strain at POI-2 ($\sigma_{norm.pt2}$) is calculated from the following equation: $\sigma_{norm.pt2}=\sigma_{pt2}/\sigma_{pt1}$, where σ_{pt2} and σ_{pt1} represent the strain at POI-1 and POI-2. Similar to normalized strain at POI-4, the calculation is based on $\sigma_{norm.pt4}=\sigma_{pt4}/\sigma_{pt3}$ (Supplementary Figure 1).

2.14. Histological processing

Whole IVDs with intact BEPs were fixed in 10 % neutral buffered formalin (Leica Biosystems, Nussloch, Germany) for 1 week, prior to EDTA decalcification in 20% w/v EDTA pH 7.4 on a shaking platform at 4 °C for approximately 3 months, with EDTA replenished twice weekly. Discs were then processed to paraffin wax. Following processing tissue samples were cut sagittally. Photographic images were captured to enable approximate macroscopic grading using Thompson grading [79], and embedded in extra-large cassettes. Seven-micron sections were cut with the aid of Sellotape™ sectioning and mounted onto positively charged slides (Leica Biosystems, Newcastle, UK) and dried at 37 °C for at least 2 weeks prior to staining.

2.15. Histological staining

Following an initial 30-minute incubation in chloroform to remove the Sellotape™ from sections, tissue sections were dewaxed in Sub-X (3 × 5mins) and rehydrated in IMS (3 × 5mins) prior to rehydration in running tap water for 5 mins. Sections were then stained with Haematoxylin and Eosin, Masson Trichrome and Alcian Blue, as described previously [61]. Histological grade of degeneration was assessed across the whole disc using previously published criteria, with separate grades calculated for NP, AF, CEP and BEP regions [71] Note that, due to washing of bony end plates prior to culture, the cellularity grading for BEPs was excluded from the grading; as such the maximal grade of degeneration was 33 [71]. Histological images were also qualitatively assessed to investigate tissue integration of NPgel, and identification of NPgel and cellularity within NPgel.

2.16. Immunohistological staining

Immunohistochemistry (IHC) was used to determine the cellular expression of key anabolic and catabolic features of disc degeneration within human tissue explants cultured for 6 weeks alone or following injection of NPgel with or without BMPCs, and in whole organ cultures of IVDs cultured for 4 weeks in a physiological loading system. Extracellular matrix proteins characteristic of the IVD: Aggrecan, Collagen type II and Collagen type I were investigated across the NP, AF and CEP tissue regions within organ cultures, and Aggrecan and Collagen type II investigated within NP tissue explants. Whilst expression of matrix degrading enzymes (MMP3, MMP13 and ADAMTS4) was investigated within the NP tissue explants and MMP3 and ADAMTS4 investigated in the NP tissue region of the IVD organ cultures. Furthermore, within tissue explants IL-1 expression was investigated as a key plethoric cytokine for disc degeneration. IL-1 was also investigated alongside IL-8 within

Table 4
List of antibodies and methods used for immunohistochemistry (IHC) experiments in this study. All secondary antibodies used at a dilution of 1:500. All antibodies purchased from Abcam.

Target	Clonality	Dilution	Antigen retrieval method	Secondary antibody
Collagen type II (ab34712)	Rabbit polyclonal	1:200	Enzyme	Goat anti rabbit (ab6720)
Aggrecan ab3778)	Mouse monoclonal	1:100	Heat	Rabbit anti mouse (ab6727)
Collagen Type I (ab90395)	Mouse monoclonal	1:200	Enzyme	Rabbit anti mouse (ab6727)
MMP3 (ab53015)	Rabbit polyclonal	1:400	Enzyme	Goat anti rabbit (ab6720)
MMP 13 (ab39012)	Rabbit polyclonal	1:200	Heat	Goat anti rabbit (ab6720)
ADAMTS4 (ab185722)	Rabbit polyclonal	1:200	None	Goat anti rabbit (ab6720)
IL-1β (ab9722)	Rabbit polyclonal	1:100	Heat	Goat anti rabbit (ab6720)
IL-8 (ab7747)	Rabbit polyclonal	1:100	Heat	Goat anti rabbit (ab6720)

the NP region of organ cultures. IHC was performed as previously reported [80] using antibodies stated in Table 4. All cells within the tissue region of interest (NP, AF or CEP) were counted as either immunopositive (brown staining) or immunonegative (only purple nuclei staining) until a total of 200 cells per sample had been counted. Counting was performed on cells throughout the entirety of the tissue region irrespective of their locality within NPgel, to determine the number of cells expressing each protein across the whole NP region. The percentage of immunopositive NP cells (for each target) was then determined.

2.17. Statistical analysis

All statistical analysis was performed using Prism 9.0 software (GraphPad Software, Inc., La Jolla, CA). Normality testing was performed to determine normality. For MRI quantification and biomechanical analysis, One-way ANOVA followed by Tukey multiple comparisons posthoc tests were performed. Macroscopic and histological grades of degeneration and immunohistochemical data were assessed with the Kruskall Wallis and Dunns post hoc test. Adjusted P values are reported to two decimal figures in all cases and $P \leq 0.05$ were considered statistically significant. Data is presented as individual data points and median.

3. Results

3.1. NPgel promotes matrix production and inhibits catabolic proteins in degenerate human tissue explants

Immunopositive staining for Aggrecan was mainly observed as cellular staining (Supplementary Figure 2), as seen previously for this antigen [80], with increased staining particularly within pericellular regions in those explants injected with NPgel and NPgel with BMPCs (Supplementary Figure 2), with a significant increase in Aggrecan immunopositive cells seen in explants injected with NPgel together with BMPCs ($P = 0.02$) (Fig. 1). Whilst an increase was also seen in NPgel alone injected explants this failed to reach significance ($P = 0.20$) (Fig. 1). Immunopositive staining for Collagen type II was seen within the tissue matrix and co-localised to cells across all explant groups, an increase in percentage of immunopositive cells was seen in both NPgel and NPgel plus BMPCs injected discs this only reached significance where BMPCs were included ($P = 0.03$) (Fig. 1), where an increase in pericellular collagen type II was evident (Supplementary Figure 2). Immunopositive staining for IL-1 was observed in non-injected tissue explants, which was decreased in explants injected with NPgel alone or with NPgel in combination with BMPCs, although this only reached significance in NPgel alone explants ($P = 0.04$) (Fig. 1& Supplementary Figure 2). Matrix degrading enzymes MMP3, MMP13 and ADAMTS4 were expressed within non-injected controls (Supplementary Figure 2), percentage immunopositivity for all matrix degrading enzymes was decreased following injection of NPgel alone or NPgel in combination with BMPCs, which was significant for MMP3 and ADAMTS4 (MMP 3: (NPgel $P = 0.02$; NPgel+BMPCS $P = 0.03$); ADAMTS4: NPgel $P = 0.003$; NPgel+BMPCs $P = 0.002$), but failed to reach significance for MMP13 (NPgel $P = 0.44$; NPgel+BMPCs $P = 0.09$) (Fig. 1).

3.2. NPgel can be injected into whole human IVDs ex vivo

Pre-warmed NPgel (~38–39 °C) was easily injected into whole human IVDs using a 25 G needle, NPgel could be visualized to fill cracks and fissures during injection via the use of Iohexol and fluoroscopic visualization (Supplementary Video 1). The total volume of NPgel injected across 8 discs ranged from 600 to 1000 µl (Mean= 890 µl, SD=150). Following injection, NPgel could be visualized to have filled natural cracks and fissures within the native human IVDs, appearing white on MRI imaging (Fig. 2A).

3.3. NPgel increases disc height and improves mechanical strength

Previously frozen human IVDs were used to test the effect of NPgel on immediate disc height change and mechanical properties of the disc. Injection of NPgel resulted in a significant increase (up to 31 %, Mean=13 %) in disc height of post-injected discs when compared to their height before the injections ($P = 0.008$) (Fig. 2B). Young's modulus was determined for each disc pre- and post-injection during simulated walking. Young's modulus was significantly increased in 6 out of 8 of the IVDs injected with NPgel with an increase in Young's Modulus between 106 and 129 % mean increase ($P<0.05$) (Fig. 2C). During failure testing, the maximum compressive strength was between 2.3 MPa and 4.1 MPa (Fig. 2D), with failure visible with a dip in the load readout (Fig. 2E). One disc herniation was induced during failure testing, which resulted in the lowest maximal compressive strength (Red point Fig. 2D& Fig. 2F), although NPgel was not extruded in any IVD (Supplemental Videos 2–3).

3.4. Ex vivo organ culture of freshly extracted cadaveric IVDs with intact boney end plates retains cell viability

For *ex vivo* study, intact freshly extracted cadaveric lumbar spines were radiographed and discs with degeneration grade 1 or 2 were selected for this study (Table 3). Discs were excised together with a thin layer of adjacent bony end plate, which prior to washing showed blockage of trabeculae (Supplementary Figure 3A). Extensive washing cleared the trabecular pores (Supplementary Figure 3B). Following 4 weeks of physiological loading, clear cells were observed within the NP (Supplementary Figure 3C), the AF (Supplementary Figure 3D) and within both the CEP and BEP (Supplementary Figure 3E). Assessment of metabolic activity comparing loaded and unloaded discs demonstrated higher metabolic activity in both the NP (2559 ± 498; $p < 0.0001$) and iAF (1873 ± 498; $p = 0.002$) in loaded compared to unloaded IVDs (Supplemental Figure 3F).

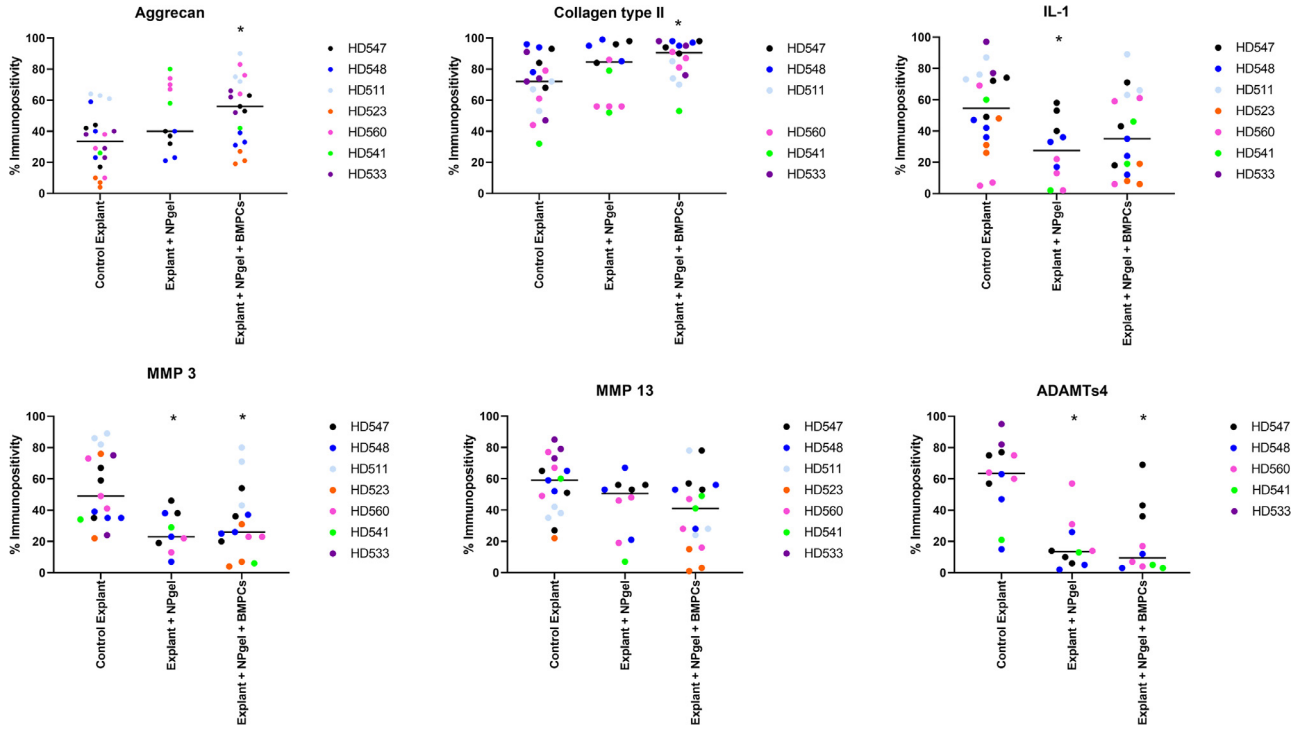

Fig. 1. Immunohistochemistry quantification for aggrecan, collagen type II, IL-1, MMP 3, MMP 13 and ADAMTS 4 within human NP tissue explants following injection of NPgel alone or in combination with BMPCs together with untreated control explants following culture for 6 weeks. Individual patient data shown as differential colours. Grand Median shown for data sets. *Indicates $P<0.05$.

3.5. NPgel alone and BMPCs seeded within NPgel injection enhance mechanical properties and maintain tissue stability of degenerate human discs

Discs injected with NPgel or NPgel + BMPCs were compressed to a greater extent during loading cycles which reached significance for NPgel alone (NPgel 1st 2 hr load $P = 0.001$; 2nd 2 hr load $P = 0.002$) (Fig. 3A). However, this change failed to reach significance in discs injected with NPgel combined with BMPCS compared to non-injected discs (1st 2 h load $P = 0.06$; 2nd 2 h load $P = 0.06$)(Fig. 3A). Whilst during relaxation periods of 0.1 MPa rest periods, discs injected with NPgel alone showed significantly greater disc height recovery than control discs during both 6 h ($P = 0.006$) and 14 h ($P = 0.0001$) rest periods (Fig. 3A). This increased swelling effect was also seen for discs injected with NPgel + BMPCs, which reached significance after the 14 h rest period ($P = 0.007$), but failed to reach significance after the 6 h rest period ($P = 0.21$) (Fig. 3A). The observed increase in loss and gain in height (compression at 2 h and re-swell at 6 h and 14 h) in the injected discs indicated that NPgel injection improved the disc tissue swell/re-swell properties. Further analysis of IVD mechanical properties was assessed at various time points throughout the culture. At an early culture period of 7 days, NPgel injection increased the stiffness of the IVD. Although this failed to reach significance to control discs ($P = 0.25$), a significant increase was seen compared to discs injected with NPgel combined with BMPCs ($P = 0.01$) (Fig. 3B). However, following 28 days in culture, the stiffness of NPgel injected discs was no different to non-injected controls, whilst those discs injected with NPgel together with BMPCs showed a significant decrease in stiffness compared to control ($P = 0.001$) and NPgel alone injected discs ($P = 0.02$) (Fig. 3C). Similarly, the modulus of discs injected with NPgel combined with BMPCs was significantly decreased following 7 days in culture, compared to control non-injected discs ($P = 0.0003$), and discs injected with NPgel alone ($P = 0.003$) (Fig. 3D), which was maintained for the 28 days in culture (NPgel +BMPCs v/s control $P = 0.001$; NPgel + BMPCs v/s NPgel $P = 0.047$) (Fig. 3E), whilst discs injected with NPgel alone displayed a small non-significant decrease in modulus at both time points (7 day $P = 0.44$) (Fig. 3D) (28 day $P = 0.20$)(Fig. 3E). The range of motion was not affected by the injection of NPgel alone or in combination with BMPCs (Figure 3F&G), a small but non-significant decrease in dissipated energy was seen following NPgel injection alone (7 day $P = 0.11$; 28 day $P = 0.22$) (Fig. 3H&I). However, the injection of both NPgel alone or NPgel combined with BMPCs decreased the normalised creep strain of discs following both 7 days (NPgel $P = 0.025$; NPgel+BMPCs $P = 0.025$) (Fig. 3J) and 28 days of culture (NPgel $P = 0.003$; NPgel+BMPCs $P = 0.005$) (Fig. 3K).

3.6. NPgel with or without the addition of BMPCs improved T1ρ MRI scan values and increased matrix deposition in ex vivo culture of live human degenerate discs

T1ρ-weighted MRI images showed darker regions with higher red intensity in discs post NPgel and cell injection in NP and iAF regions. Clear regions corresponding to proteoglycan loss were observed in non-injected discs post-culture (Fig. 4A). Quantification of the same pre- versus post-culture ROIs in the MRI scans of NP area showed a significant increase in T1ρ value of injected discs with NPgel alone from 14,378.7 ± 59.3 to 15,805.7 ± 295.7 ($p = 0.017$) (Fig. 4B) and with BMPCs- seeded NPgel from 14,313.9 ± 1708.2 to 15,885.4 ± 2070.5 ($p = 0.02$) (Fig. 4B). There was a non-significant increase in T1ρ values when comparing the same iAF ROI scans in the pre- to the post-culture scans in both NPgel (from 9048.2 ± 1000.3 to 9811.8 ± 1280.6; $p = 0.96$) and NPgel+BMPCs (from 8000.4 ± 986.6 to 8728.2 ± 1056.4; $p = 0.95$) injected discs. The observed loss in average intensity, when we compared the same ROIs in MRI scans before after the culture of non-injected discs, was not significant in NP (pre 12,707.08 ± 922.9 and post 11,734.21 ± 1052.1; $p = 0.11$) and iAF (pre 8371.9 ± 738.1

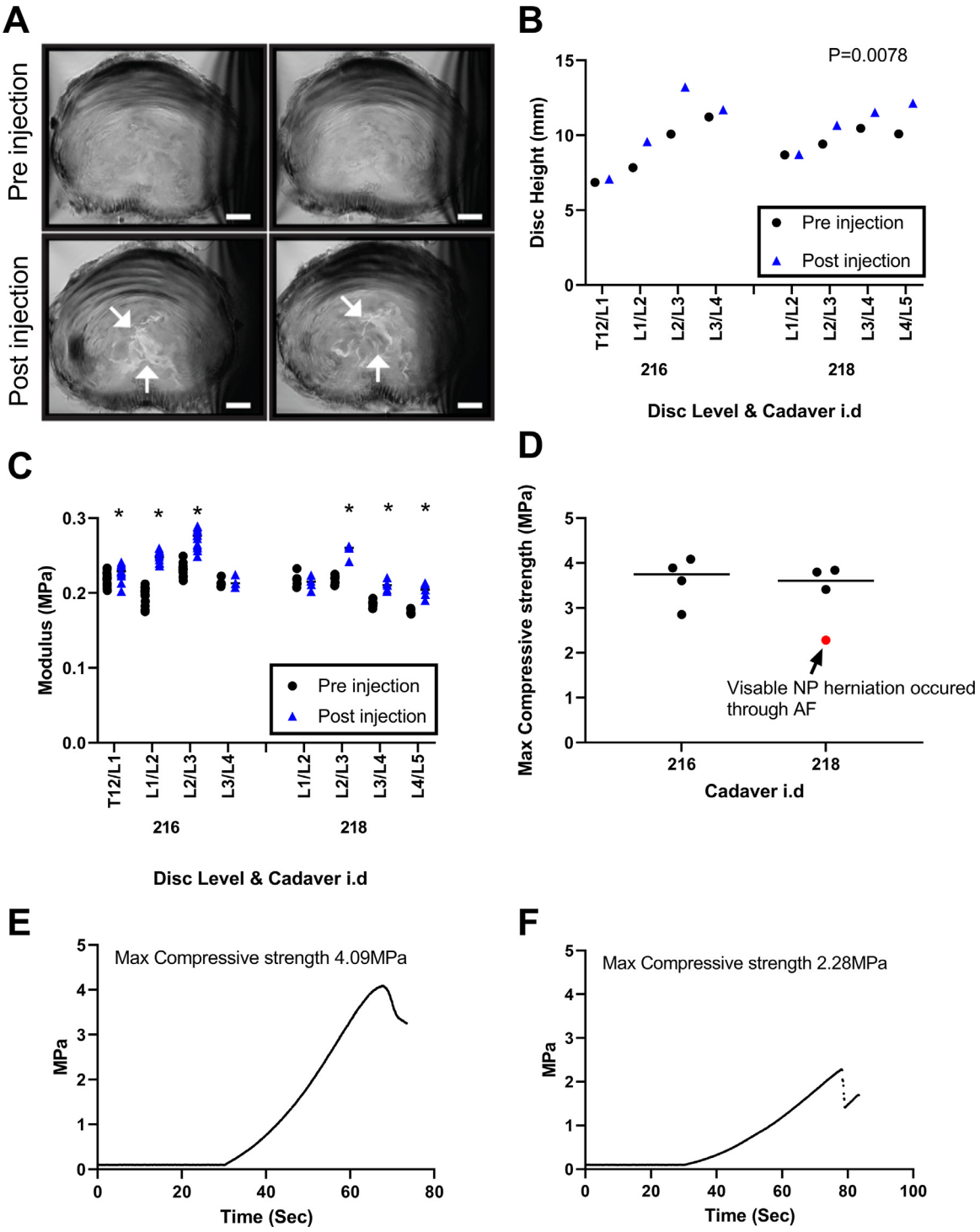

Fig. 2. **(A)** MRI images showing pre and post-injection of NPgel into whole cadaveric human IVDs, scale bar = 5 mm. (B) Cadaveric human IVDs were examined via X-ray to determine IVD height pre and post-injection of NPgel (600–1000μl) with a significant increase in disc height observed in the injected discs $P = 0.0078$. (C): Whole discs were loaded under a compressive loading regime to mimic walking and Youngs moduli were calculated pre and post-injection with NPgel. NPgel injection resulted in a significant increase in Youngs moduli of discs in 6 out of 8 discs injected (*indicates $P<0.05$). (D): Maximum compressive strength tested by compression (2 mm/min) until failure. Discs failed at 2–4 times the maximal physiological load with a maximal failure strength of 4.09 MPa. (E): Failure testing data for the disc with the highest compressive strength. (F) Failure testing data for the disc with the lowest compressive strength, where visible NP herniation occurred through the AF (although NPgel was not extruded). ($n = 8$).

and post 7361.59 ± 735.7; $p = 0.75$) ROIs (Fig. 4B-C). The gain of percentage in MRI signal (red color intensity) following culture was significant in the NP area of NPgel (9.91 ± 1.82 %; $p = 0.015$) and NPgel+BMPCs (10.75 ± 3.89 %; $p = 0.016$) injected discs when compared the same ROIs before the culture (Fig. 4D). MRI of non-injected control discs following the culture showed a decrease (−7.99 ± 2.12 %) when compared to the same NP region of interest before the culture, but significance was not reached (Fig. 4D). Comparison of the T1ρ values in the same ROI of iAF MRI scans showed non-significant differences between before and after cul-

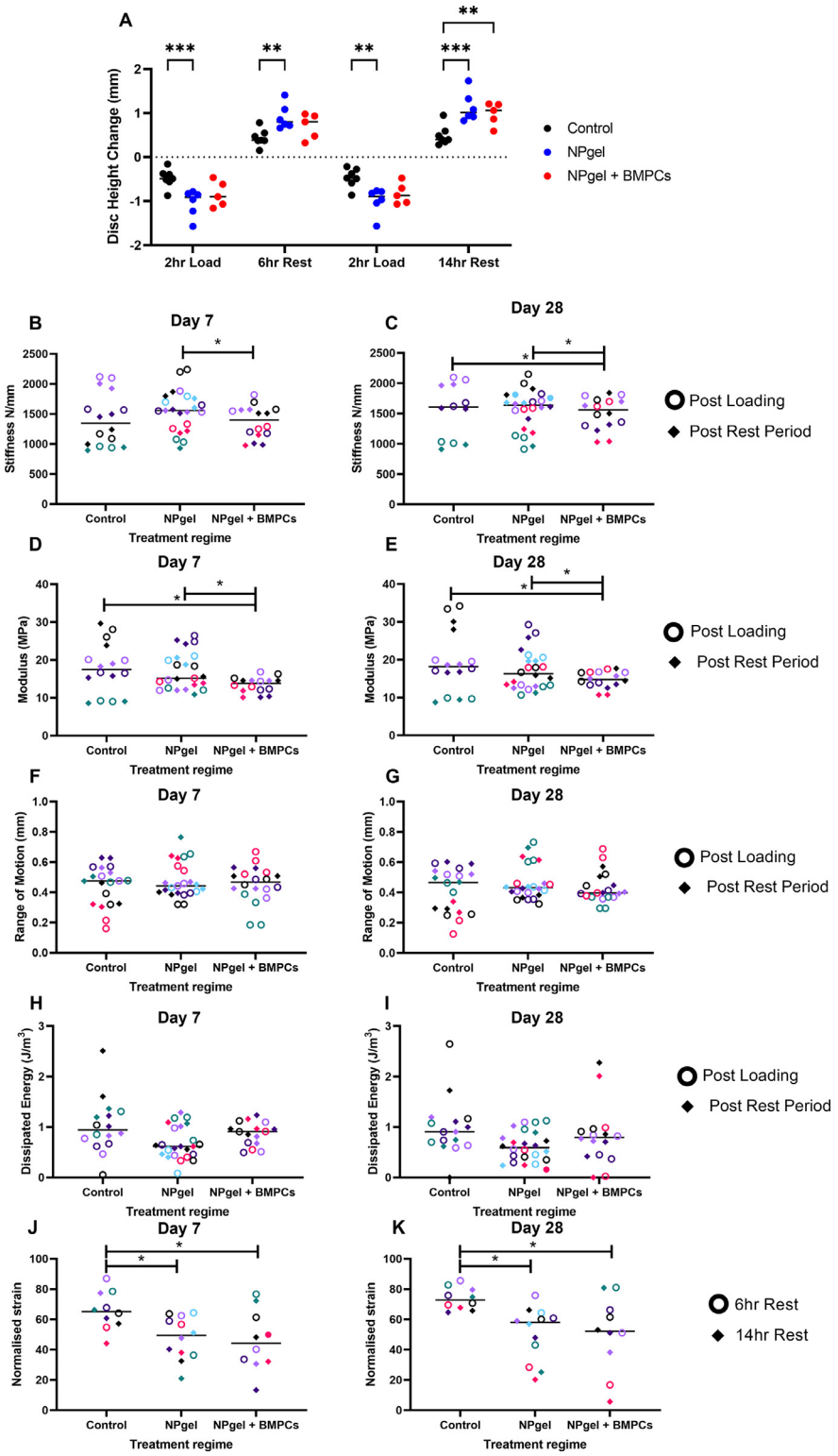

Fig. 3. Biomechanical analysis of organ culture of whole human IVDs either left uninjected (control), or injected with NPgel alone or in combination with BMPCs. Whole discs were cultured under physiological loading for 28days, with in line biomechanical analysis performed. (A) Disc height change in mm from pre-culture disc height following 2 hrs dynamic loading 0.1MPa-0.6 MPa 0.1 Hz, 6hr rest at 0.1 MPa static culture, 2 hrs dynamic loading 0.1MPa-0.6 MPa 0.1 Hz, and a final 14hr rest period. Data shown is the averaged disc height changes over the 28days of culture during each loading cycle. (B) Stiffness (N/mm) following 7days of culture measured post 2hr loading cycles (circles) and rest periods (6 &14hr) (diamonds). (C) Stiffness (N/mm) following 28days of culture measured post 2hr loading cycles (circles) and rest periods (6 &14hr) (diamonds). (D) Modulus (MPa) following 7days of culture measured post 2hr loading cycles (circles) and rest periods (6 &14hr) (diamonds). (E) Modulus (MPa) following 28days of culture measured post 2hr loading cycles (circles) and rest periods (6 &14hr) (diamonds). (F) Range of Motion (mm) following 7days of culture measured post 2hr loading cycles (circles) and rest periods (6 &14hr) (diamonds). (G) Range of Motion (mm) following 28days of culture measured post 2hr loading cycles (circles) and rest periods (6 &14hr) (diamonds). (H) Dissipated energy (J/m^3) following 7days of culture measured post 2hr loading cycles (circles) and rest periods (6 &14hr) (diamonds). (I) Dissipated energy (J/m^3) following 28days of culture measured post 2hr loading cycles (circles) and rest periods (6 &14hr) (diamonds). (J) Normalised strain (%) following 7days of culture measured post 2hr loading cycles (circles) and rest periods (6 &14hr) (diamonds). (K) Normalised strain (%) following 28days of culture measured post 2hr loading cycles (circles) and rest periods (6 &14hr) (diamonds). B-K each disc shown in differential colours. * indicates $P<0.05$.

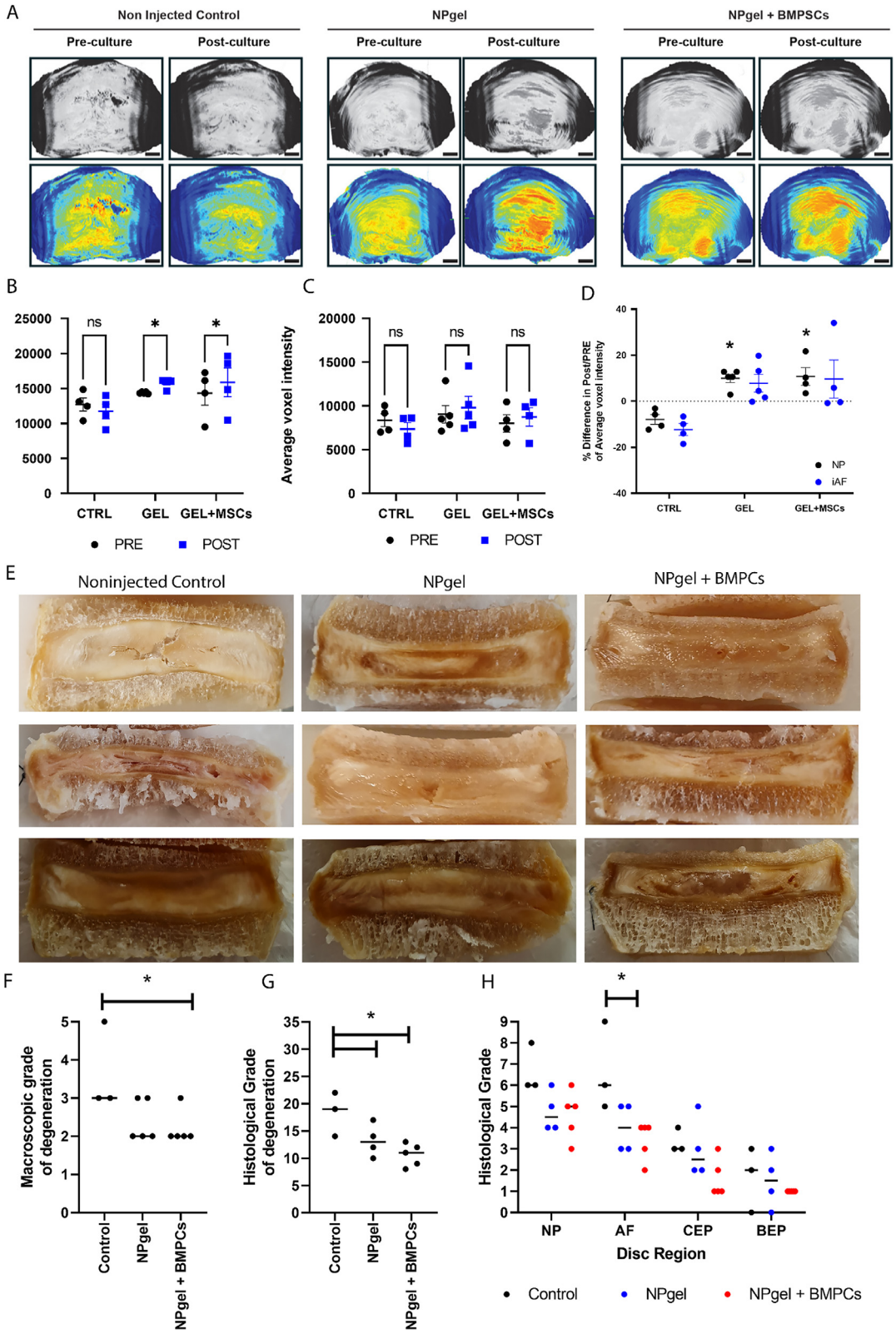

Fig. 4. (A): Representative images of mid-axial T1ρ slices pre-culture and the same location after 28 days in non-injected (CTRL), NPgel, or NPgel+hMSCs injected discs. The heatmap correlates the red color with the highest and the blue color with the lowest T1ρ values, scale bar = 5 mm. (B) Quantification of ROIs for NP (Average Voxel intensity) and (C) AF regions (Average voxel intensity) in the three groups showed significant enhancement in the ROIs of NP area for the NP gel and NPgel+hMSCs injected discs following the culture. (C) Summary graph showing percentage change in T1ρ values post-normalized to their respective pre-culture scans in injected and non-injected discs. (E) Macroscopic images of whole human IVDs following 28days culture within non-injected controls, discs injected with NPgel alone and NPGel +BMPCs. Discs were fixed, EDTA decalcified and embedded to paraffin wax prior to transverse sectioning and macroscopic images captured of whole discs. NPgel can be clearly seen in discs injected with NPgel. (F) Macroscopic grade of degeneration (Thompson grading scheme). (G) Overall histological grade of degeneration (Le Maitre grading scheme) and (H) sub grades for each disc region across the IVD. Note each region is scored out of 9 except the BEP where cellularity score was not possible and thus total score for BEP is 6. * indicates $P<0.05$. (For interpretation of the references to colour in this figure legend, the reader is referred to the web version of this article.)

ture in all discs (Fig. 4D). These results indicated that treatment of human IVDs with BMPCs-seeded NPgel and NPgel alone increased the T1ρ values within NP area of human IVDs following 28 days of dynamic culture.

3.7. NPgel with or without the addition of BMPCs decreases macroscopic and microscopic grade of degeneration

Macroscopic visualization of cadaveric human IVDs following 4 weeks in culture within the loaded disc culture system demonstrated clear cracks and fissures within untreated controls (Fig. 4E). Within discs where NPgel had been injected, visible regions of gel could be visualised particularly within cracks and fissures in the NP region (Fig. 4E). Discs injected with NPgel either with or without BMPCs appeared similar (Fig. 4E). Macroscopic grading of discs demonstrated a significant decrease in macroscopic degeneration within discs injected with NPgel together with BMPCs ($P = 0.04$) (Fig. 4F). A decrease was also seen for NPgel alone, although this failed to reach significance ($P = 0.14$) (Fig. 4F). Following histological staining of discs and grading according to the standardized histological grading scheme for human discs[71], with the exclusion of BEP cellularity due to the washing performed on discs prior to culture, a significant decrease in histological grade of degeneration could be seen following both NPgel injection alone ($P = 0.0006$), and when NPgel was injected together with BMPCs ($P<0.0001$) (Fig. 4G), with a decrease in grade of degeneration seen across all regions of the disc (Fig. 4G), reaching significance within the AF for NPgel where BMPCs were injected together ($P = 0.03$) (Fig. 4H). Within non-injected control discs, histological staining demonstrated fissures within the NP (Fig. 5A) along with the presence of granulation tissue (Fig. 5B). Fissures were also seen within the AF tissue regions (Fig. 5C). NP cells appeared as multicellular clusters with weak Masson trichrome collagen staining (Fig. 5D), whilst the CEP cells were evenly distributed through the endplate with proteoglycan staining with alcian blue localized to the cells (Fig. 5E). Within IVDs injected with NPgel, some fissures within the NP tissue remained void (Fig. 5F), whilst others contained clear NPgel within the fissures (Fig. 5G). Fissures within the AF were also seen to contain NPgel (Fig. 5H), which stained strongly for alcian blue (Figure 5I&J). In discs injected with NPgel with BMPCs, again fissures within the NP tissue were filled by gel, with both small (Fig. 5K), and large fissures (Fig. 5L) demonstrating the presence of NPgel. An increase in cellularity was observed around NPgel in NPgel + BMPCs injected discs adjacent to fissures across the tissue (Fig. 5M). Strong alcian blue staining was seen in NPgel filled regions in the NP and AF (Fig. 5N &O).

3.8. NPgel with or without BMPCs promotes production of matrix synthesis and decreases catabolism within whole human IVDs following 4 weeks of organ culture

Collagen type I immunopositive staining was predominantly found within the AF and CEP of all discs and no difference was seen following injection of NPgel alone or in combination with BMPCs ($P>0.05$) (Supplementary Figure 4 & Fig. 6). Collagen type II immunopositive staining was seen within the NP at low levels in two out of the three control non-injected discs, but at high levels in one control non-injected disc with an apparent increase seen in the NP region following NPgel injection either alone or in combination with BMPCs although this failed to reach significance ($P>0.05$) (Fig. 6& Supplementary Figure 5). Collagen type II immunopositivity was also slightly increased within the AF tissue of NPgel and NPgel +BMPC injected discs, although this failed to reach significance ($P>0.05$) (Fig. 6& Supplementary Figure 5). Collagen type II immunopositivity was high in all discs within the CEP region (Fig. 6& Supplementary Figure 5). Aggrecan immunopositivity was expressed at low levels across all regions of the disc in control non-injected discs, whilst within the NP region of NPgel injected with or without BMPCs an apparent increase in number of cells immunopositive for Aggrecan was seen compared to control discs, although this failed to reach significance ($P>0.05$) (Fig. 6& Supplementary Figure 6). The catabolic matrix degrading enzymes MMP 3 and ADAMTS 4 were expressed within the NP region of the control non-injected discs and the number of immunopositive cells were significantly decreased following NPgel injection ((MMP 3 $P = 0.005$), (ADAMTS 4 $P = 0.02$)) (Fig. 7& Supplementary Figure 7). A similar trend of decreased immunopositivity staining for MMP 3 and ADAMTS 4 was also seen following NPgel injection with BMPCS although this failed to reach significance ((MMP3 $P = 0.41$), (ADAMTS4 $P = 0.10$)) (Fig. 7& Supplementary Figure 7). Immunopositive staining was also seen in control non-injected discs for IL-1 and IL-8, with expression decreased following injection of NPgel and NPgel + BMPCs which reached significance following NPgel injection for IL-1 ($P = 0.006$), and IL-8 for NPgel + BMPCs ($P = 0.01$) (Fig. 7& Supplementary Figure 7). Whilst the decreases seen in IL-1 in NPgel + BMPCs failed to reach significance ($P = 0.33$), or IL-8 in NPgel injected discs ($P = 0.20$) (Fig. 7& Supplementary Figure 7).

4. Discussion

Regeneration of the IVD is an attractive prospect for the treatment of LBP associated with disc degeneration. Several approaches have been proposed to date, yet the development of new therapies for the regeneration of the degenerate IVD is complicated by the lack of validated large bipedal animal models that mimic the human spinal anatomy, the naturally occurring IVD degeneration, and the human genetic background [59]. Long-term organ culture models can bridge this gap and provide human *in vivo*-like conditions for studying therapeutic candidates [64,66,81]. Here, several key questions essential to support translation to the clinic of a prospective regenerative injectable biomaterial (NPgel) were investigated using human IVD tissues. NPgel could be easily injected into naturally degenerate human IVDs, filling natural cracks and fissures and leading to an immediate increase in disc height and Young's modulus. Furthermore, NPgel was retained both during failure testing of previously frozen discs and during long term 4-week culture in an organ culture system under physiological load. Injection of NPgel alone or in combination with BMPCs increased MRI signal intensity, decreased macroscopic and microscopic grade of degeneration and promoted normal matrix protein expression and inhibited catabolic cytokines and matrix degrading enzymes. Furthermore, biomechanical properties were improved in NPgel injected discs with restoration of compression and swelling capabilities during diurnal loading and decreased creep strains, with effects seen early in the culture cycle and maintained for the 28 days investigated. These results provide essential proof of concept data supporting the use of NPgel as an injectable therapy for disc regeneration.

Using whole human discs this study was able to demonstrate the facile injection of NPgel through a 25 G needle, where the biomaterial flowed easily into natural cracks and fissures within the disc, due to the low viscosity of NPgel prior to gelation [60]. The injection through a fine bore needle shows a major advantage over other more viscous gel systems which require wider bore needle injection [56,82–85], or nuclectomy prior to application [86]. Furthermore, viscous gel systems often appear as a bolus within discs following injection [51], which can also lead to failure under load [51,52,86]. The use of fine bore needles for injection into the IVD is also essential to prevent damage to the annulus fibrosus and the potential induction of degeneration[59]. The

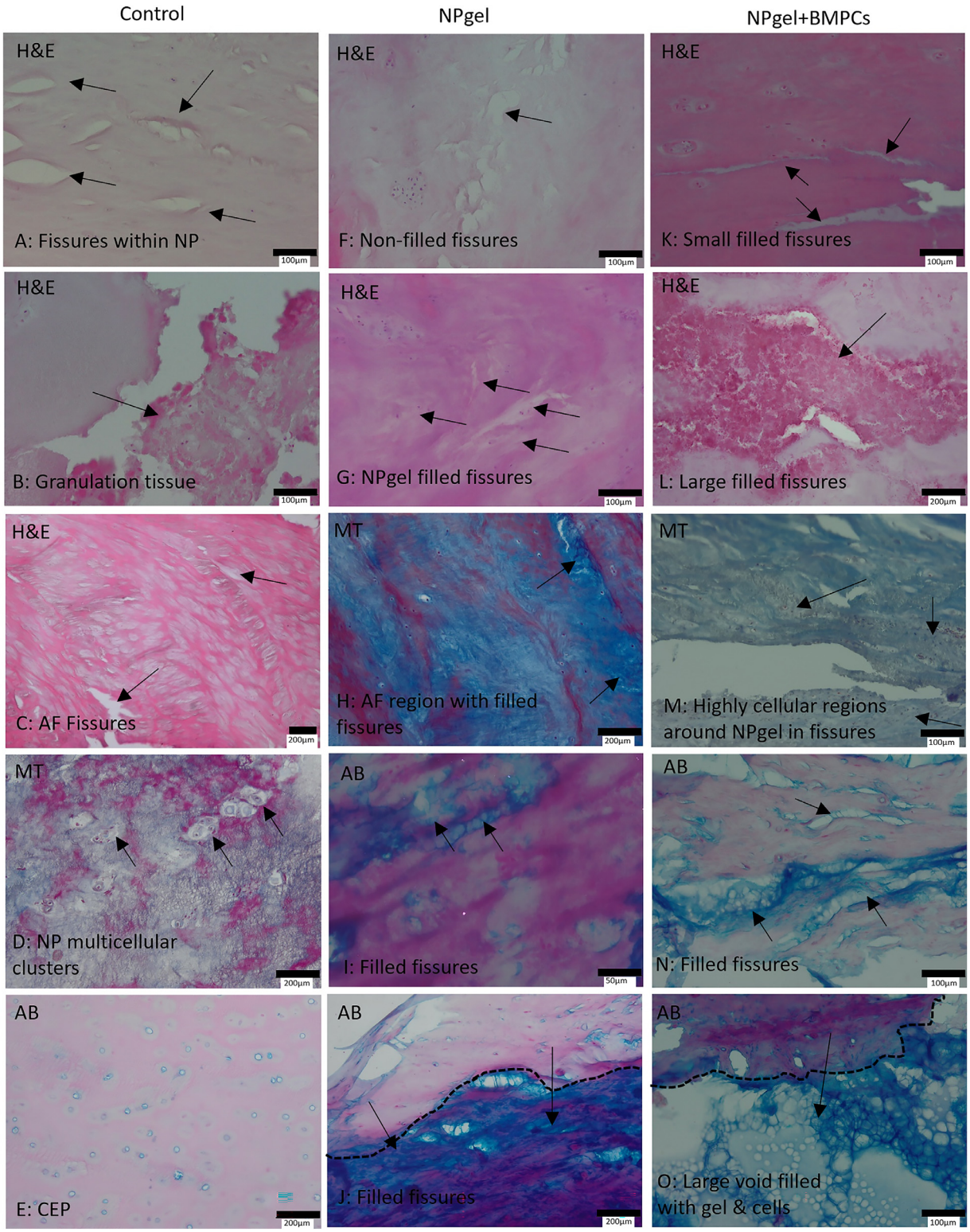

Fig. 5. Histological staining of intervertebral discs cultured for 28days under physiological load within A-E: Non-injected control discs, F-J: NPgel alone injected discs and K-O: Discs injected with NPgel in combination with BMPCs. Key features indicated images demonstrating A: Fissures within the NP; B: Granulation tissue; C: AF fissures; D multicellular clusters and E: CEP within non-injected controls. F: Non filled and G Filled fissures within the NP and H,I & J the AF filled with NPgel in NPgel injected discs. K: Small filled and L large filled fissures with regions of high cellularity around fissures (M) and regions of disc filled with NPgel and cells within cracks (N) and large voids (O) of the disc. Histological stains included Haematoxylin and Eosin (H&E), Masson Trichrome (MT) and Alcian Blue (AB). Scale bars as indicated on images. (For interpretation of the references to colour in this figure legend, the reader is referred to the web version of this article.)

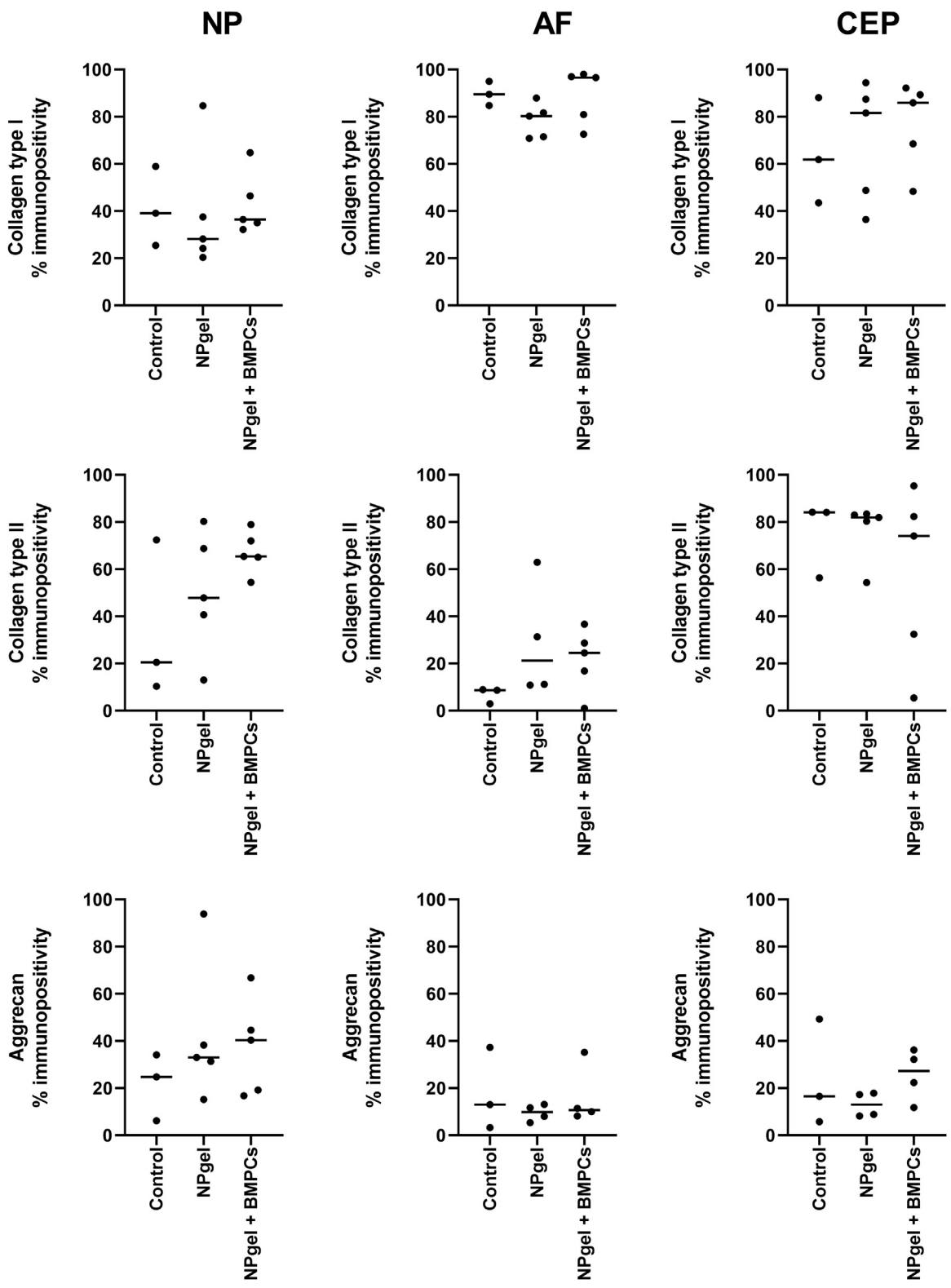

Fig. 6. Percentage of immunopositive cells for collagen type I, collagen type II and aggrecan within the NP, AF and CEP regions of the disc either left untreated, or injected with NPgel alone or in combination with BMPCS and cultured in organ culture under physiological load for 28days. * indicates $P<0.05$.

use of a 25 G needle did not induce disc degeneration in smaller discs isolated from goats, beagles and bovine caudal IVDs [87–89]. Moreover, in a prospective uncontrolled clinical study, insertion of a 18 G needle into the central NP did not accelerate degeneration [90]. In the current study initial investigations using previously frozen human discs demonstrated that naturally degenerate discs were able to be injected with volumes of between 600 and 1000 µl of NPgel, this is similar to that seen in a clinical study where 900 µl of an ethanol gel (DiscoGel) which was injected into the NP of degenerated discs [90]. Within the current study an im-

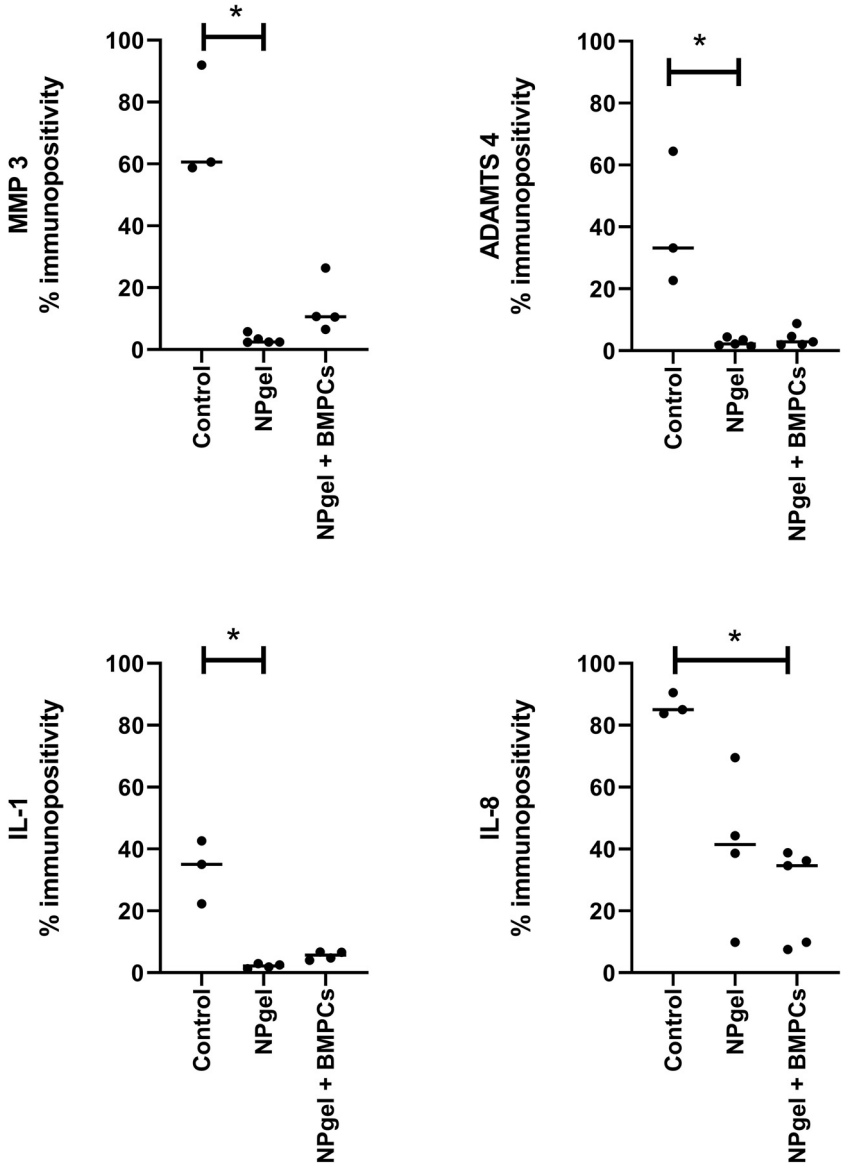

Fig. 7. Percentage of immunopositive cells for MMP 3, ADAMTS 4, IL-1 and IL-8 within the NP region of the discs either left untreated, or injected with NPgel alone or in combination with BMPCS and cultured in organ culture under physiological load for 28days. * indicates $P<0.05$.

mediate increase in disc height was observed following injection of NPgel, which is likely due to the filling of cracks and fissures and increased disc volume following injection as seen in other studies [56,85]. Although these studies were performed on non-loaded discs they were performed within whole motion segments at atmospheric pressure which is 0.1 MPa, and as loads during supine have been reported to be 0.1MPa [14] this would mimic injection whilst supine and thus additional load application was not necessary during injection. Within the organ culture investigation, the volume injected was limited to 500 µl to ensure a standardised volume was included in all discs, however this did result in incomplete filling of void spaces evident with macroscopic and microscopic imaging of discs following harvest. However, for clinical application it would be envisaged that NPgel would be injected until there was a back pressure, thus filling all the cracks and fissures within the disc. As NPgel has mechanical properties which matches that of native NP tissue [60]. Thus, the filling of the cracks within the degenerate disc which result in the heterogeneous distribution of load bearing forces across the disc, negatively impacting on cell behaviour would be corrected resulting in a more homogeneous distribution of load across the disc once cracks and fissures have been filled.

The IVD is an important load-bearing joint where the aggrecan rich NP, within a healthy IVD, provides a high fixed charge density creating high osmotic pressure within the tissue, which is essential for normal biomechanical function of the IVD [10,11,91]. During axial compression during diurnal loading the external loads are higher than the internal swelling stress provided by the osmotic pressure of the NP tissue, resulting in the flow of water out of the disc and a subsequent decrease in disc height. Whilst during night-time rest the external axial compression is reduced and the internal swelling stress exceeds the external stress, and thus fluid flows back into the disc [11,13]. This fluid flow during diurnal loading of the IVD is essential to maintain nutrient supply to the disc and the removal of waste products [11]; during disc degeneration the reduction in proteoglycans, results in decreased fixed charge density and swelling pressure results in abnormal solute diffusivity [11,92]. Within the current study naturally degenerate whole human IVDs displayed decreased disc height during dynamic loading which increased again during rest periods, with a greater re-

covery rate seen during 14 h recovery v/s 6 h recovery, mimicking the disc height changes seen in vivo during normal diurnal loading. Injection of either NPgel alone or in combination with BMPCs resulted in an increased compression of the disc during dynamic loading and significantly greater disc swelling during 14 h recovery mimicking disc height increase seen during night-time rest. This was further confirmed with the decreased normalised creep strain seen in NPgel +/- BMPCs injected discs to non-injected degenerate discs. Normalised creep strain has been seen previously to increase within degeneration [93], and nucleotomy models increased creep strain by over 40 %[94], sham treated discs further increased creep strain [95], whilst injection of a triple interpenetrating network hydrogel (which is composed of chitosan, dextran and teleostean) reduced creep strain by 3 % compared to nuclectomy alone [95]. Whilst in the current study we saw a reduction in creep strain of ~70 % from non-injected degenerate human IVDs, demonstrating a substantial reduction in creep strain following injection of NPgel either alone or in combination with BMPCs. The decreased creep strain, increased swell/re-swell properties and increased disc height seen in the current study following NPgel injection suggests restoration of key biomechanical features essential to restore spinal motion which is essential to tackle low back pain [96]. An increase in Young's modulus was also seen in the current study when discs were injected with NPgel to fill the natural voids and fissures seen during the mechanical testing of previously frozen discs, suggesting a restoration of compressive strain which is also essential for normal spinal function [96]. The molecular mechanisms underpinning IVD tissue stiffening and degeneration is unclear because there is no direct correlation between changes in mechanical properties and structural/molecular tissue changes [97,98]. IVD mechanical responses are also sensitive to the testing environment (humidity, temperature), the methods of storage, the mechanical properties of each spinal level, the nucleus pulposus, and annulus fibrosis at varying strain rates and levels of degeneration. The compressive Young's modulus of IVDs decreases with degeneration [99,100].

However, in the discs used for the organ culture study where the implantation volume was limited to 500 µl, such an effect was not observed. Within organ culture discs, injection of 500 µl of NPgel failed to completely fill cracks and fissures as seen macroscopically following processing and histology. This incomplete filling may explain the lack of an increase in modulus of the discs and indicates the clinical requirement to ensure cracks and fissures are filled during injection. This could be aided with the use of a pressure sensor to measure internal pressure increases during injection as has been used in a goat model during injection of a triple interpenetrating network hydrogel [56], and the use of C-arm fluoroscopic guidance during injection, as used during the injection of previously frozen discs in the current study. In contrast, injection of NPgel together with BMPCs resulted in a significant decrease in Young's modulus and stiffness of whole human IVDs cultured under physiological loading, this decrease could have been a result of slightly higher matrix production, particularly aggrecan, which would result in higher water content, which was seen in discs injected with BMPCs compared to NPgel alone (although this failed to reach significance). NPgel injection however did not affect the range of motion (single plane) of the whole discs, whilst a small but nonsignificant decrease in dissipated energy was observed in discs following NPgel injection alone but not when combined with BMPCs. A decrease in dissipated energy has been observed previously following needle puncture of discs [62], whilst others have shown that needle puncture did not affect dissipated energy [101], thus this decrease may indicate some loss of dissipated energy during injection [62]. Human IVDs are known to show a decrease in energy dissipation capacity during degeneration due to matrix degradation and presence of fissures [93,102–104], and thus for complete restoration of biomechanical function one would expect an increase in dissipated energy. Although some studies have suggested an increase in energy dissipation with increased degeneration during lateral bending [105], therefore further research is needed to understand the implications of these findings. Furthermore, given that the volume of NPgel injected into discs which were used for organ culture and physiological loading was limited to 500 µl, which failed to completely fill the cracks and fissures, energy dissipation may have been increased if all void spaces were completely filled by injecting a larger volume of NPgel. In addition, organ cultures were limited to 4 weeks and whilst an increase was seen in matrix deposition, this did not reach significance, although MRI intensity was significantly increased within discs injected with NPgel alone or in combination with BMPCs. In vivo the restoration of dissipated energy could be expected to follow with increased matrix deposition which is likely to take a longer time than the 4 weeks investigated within the *ex vivo* organ culture system used here.

Interestingly, although organ cultures were limited to 4 weeks a significant decrease in both macroscopic and microscopic degeneration, which was accompanied by an increase in MRI intensity, were observed following injection of NPgel alone or in combination with BMPCs. Within human explant cultures a significant increase in both aggrecan and collagen type II immunopositive cells were seen in those explants injected with NPgel in combination with BMPCs, and whilst an increase was also seen in NPgel alone, although this failed to reach significance. Demonstrating that even BMPCs isolated from elderly individuals were able to increase matrix production following injection via NPgel into disc tissue explants. Similarly, within organ cultures an increase was seen in collagen type II and aggrecan but not collagen type I immunopositivity, although this failed to reach significance. Although it could not be determined whether the BMPCs injected via NPgel survived as it was not possible to pre label the cells for these studies. However increased cellularity was observed within regions injected with NPgel + BMPCs compared to control non-injected discs and those injected with NPgel alone, although it was not possible to quantify this cellularity. Similar increases in aggrecan and collagen type II expression have been observed following the injection of NPgel into a caprine organ culture degeneration model [63], demonstrating that the cells from native degenerate IVDs do still have the capacity to produce appropriate NP matrix. Whilst the effects seen in organ culture failed to reach significance these findings are promising at this early time course of 4 weeks. Interestingly, in a clinical trial study to assess the safety and the efficacy of a hydrogel (double cross-link microgel - DXM) injection into the intervertebral disc (IVD) space in patients with painful lumbar degenerative disc disease, has proposed that 24 to 48 weeks will be needed to evaluate the effect of the injected gel [106]. Furthermore, the current study was limited by the number of discs which could be investigated; sourcing cadaveric discs for live organ culture is limited, which was further restricted by the prior selection of grade 2 discs only for these studies. Thus, the expansion on human explants enabled increased donors to be investigated, with patient matching possible for explant culture, removing individual variability as a potential confounding factor.

In addition to effects on anabolic factors, the current study demonstrated that the catabolic cell phenotype, a characteristic of human disc degeneration [5] was inhibited in both the human explant culture system and whole organ culture. This demonstrated that NPgel injection decreased the catabolic phenotype of NP cells; this inhibition of catabolism was also observed when NPgel was injected into a degenerate caprine organ culture model which was maintained under physiological loading [63]. Whilst the inhibition of catabolic factors within both the caprine system previously [63], and the human organ culture system here could have been a re-

sult of the restoration of mechanical loading, a similar decrease in catabolic factors was also seen in the human explant culture system, suggesting that the effects are a direct result of the inclusion of NPgel, and could be due to the increased hydration and potential osmotic effect on the local cells. Whilst both NPgel alone and NPgel + BMPCs showed a decrease in catabolic factors, the effects were greater with NPgel alone, suggesting that NPgel enables the inhibition of the production of catabolic factors in native disc cells, without the need of an additional regenerative cell source. Limited studies have investigated the potential of biomaterials to inhibit the catabolic environment of the native disc, with most focusing purely on promoting matrix production [81,107–111]. Previous studies targeting the inflammatory cytokine profile of the degenerate disc have involved functionalization of hydrogels with inhibitory agents such as fucoidan within dextran hydrogels [85], epigallocatechin 3-gallate into gelatin microparticles [112], whilst Han et al., (2023) targeted reactive oxygen species to reduce inflammatory factors via incorporation of metal nanoparticles into methacrylated gelatin and hyaluronic acid [113]. Cross-linked HA systems have also been shown to inhibit neurotrophic factor expression within an IL-1 induced model of degeneration [114], and Teixeira *et al*., inhibited the action of COX-2 by loading diclofenac into chitosan poly γ-glutamic acid nanoparticles, decreasing catabolism [115]. Whilst there are several approaches investigated to date, targeted at inhibiting the catabolic signalling within the degenerate disc [116], none aim to restore biomechanics, inhibit catabolism and induce anabolism within the same system. Most have only been investigated with animal cells in vitro and have not considered approaches within human cells or within model systems more representative of native disc degeneration.

5. Conclusions

To mimic the human in vivo conditions and the unique IVD niche, we used an intact human disc culture model allowing for dynamic loading and cell viability for extended periods [67–69,107,117]. The intact disc organ culture system maintains the cells in their unique microenvironment, making their response to therapeutic strategies physiologically relevant. Our human disc culture system bridges the gap between in vitro and in vivo and provides useful proof of concept and valuable insights into the regenerative potential of NPgel for nucleus pulposus repair. This system demonstrated promising results within a short time frame, with improved biomechanics, increased MRI intensity, matrix production and decreased catabolic factors following NPgel injection. Interestingly the addition of BMPCs did not appear to provide a substantial advantage to NPgel injection alone, apart from potentially increased matrix production. Thus, longer term in vivo animal and clinical studies are now required to identify whether NPgel alone is sufficient to inhibit the degenerative cascade, restore biomechanics and induce long-lasting regeneration of the disc which tackles low back pain.

Author contributions

CS, LH and CLM, contributed to conceptualization and design of the study and contibuted to funding aquisition; LH and CLM performed project administration, HC, LL, JS, LB, CLM, contributed to acquisition of laboratory data and data curation; HC, JS, XL, CLM performed formal data analysis; HC, JS, XL, CS, JL, LB, LH, CLM contributed to formal interpretation of the data; HC and CLM generated visualization of data. HC, CLM wrote the orignal draft; All authors critically revised the manuscript for intellectual content and were involved in review and editing and approved the final version and agree to be accountable for all aspects of the work.

Declaration of Competing Interest

The authors declare the following financial interests/personal relationships which may be considered as potential competing interests: Christine Le Maitre reports financial support was provided by Versus Arthritis. Christine Le Maitre reports financial support was provided by UKRI Medical Research Council. Lisbeth Haglund reports financial support was provided by Canadian Institutes of Health Research. Christine Le Maitre reports a relationship with Orthoson Ltd that includes: consulting or advisory. Christine Le Maitre & Christopher Sammon have patents #Composite hydrogels GB2493933B, US2014219973A, EP2747797A licensed to Orthoson.

Acknowledgements

The Authors would like to thank the surgeons: Mr Ashley Cole, Mr Neil Chiverton, Mr Antony Michael, Mr Lee Breakwell, Mr Michael Athanassacopoulos, Mr Marcel Ivanov and Mr James Tomlinson from Northern General Hospital, Sheffield Teaching Hospitals NHS Trust for supply of human disc samples. Mark Wilkinson, Diane Swift and South Yorkshire and North Derbyshire Musculoskeletal Biobank for providing surgical samples for BMPCs utilised in the tissue explant component of the study. The McGill Scoliosis and Spine Group for supply of cadaveric human spines for this research. Dr Abbey Thorpe for contribution to explant culture experiments. Versus Arthritis, the Medical Research Council (UK) (MR/P026796/1) and the Canadian Institutes of Health Research (grant PJT 165995) for funding this research.

Supplementary materials

Supplementary material associated with this article can be found, in the online version, at doi:10.1016/j.actbio.2023.12.041.

References

[1] M.L. Ferreira, K. de Luca, L.M. Haile, J.D. Steinmetz, G.T. Culbreth, M. Cross, J.A. Kopec, P.H. Ferreira, F.M. Blyth, R. Buchbinder, J. Hartvigsen, A.-M. Wu, S. Safiri, A.D. Woolf, G.S. Collins, K.L. Ong, S.E. Vollset, A.E. Smith, J.A. Cruz, K.G. Fukutaki, S.M. Abate, M. Abbasifard, M. Abbasi-Kangevari, Z. Abbasi-Kangevari, A. Abdelalim, A. Abedi, H. Abidi, Q.E.S. Adnani, A. Ahmadi, R.O. Akinyemi, A.T. Alamer, A.Z. Alem, Y. Alimohamadi, M.A. Alshehri, M.M. Alshehri, H. Alzahrani, S. Amini, S. Amiri, H. Amu, C.L. Andrei, T. Andrei, B. Antony, J. Arabloo, J. Arulappan, A. Arumugam, T. Ashraf, S.S. Athari, N. Awoke, S. Azadnajafabad, T.W. Bärnighausen, L.H. Barrero, A. Barrow, A. Barzegar, L.M. Bearne, I.M. Bensenor, A.Y. Berhie, B.B. Bhandari, V.S. Bhojaraja, A. Bijani, B.B.A. Bodicha, S.R. Bolla, J. Brazo-Sayavera, A.M. Briggs, C. Cao, P. Charalampous, V.K. Chattu, F.M. Cicuttini, B. Clarsen, S. Cuschieri, O. Dadras, X. Dai, L. Dandona, R. Dandona, A. Dehghan, T.G.G. Demie, E. Denova-Gutiérrez, S.M.R. Dewan, S.D. Dharmaratne, M.L. Dhimal, M. Dhimal, D. Diaz, M. Didehdar, L.E. Digesa, M. Diress, H.T. Do, L.P. Doan, M. Ekholuenetale, M. Elhadi, S. Eskandarieh, S. Faghani, J. Fares, A. Fatehizadeh, G. Fetensa, I. Filip, F. Fischer, R.C. Franklin, B. Ganesan, B.N.B. Gemeda, M.E. Getachew, A. Ghashghaee, T.K. Gill, M. Golechha, P. Goleij, B. Gupta, N. Hafezi-Nejad, A. Haj-Mirzaian, P.K. Hamal, A. Hanif, N.I. Harlianto, H. Hasani, S.I. Hay, J.J. Hebert, G. Heidari, M. Heidari, R. Heidari-Soureshjani, M.M. Hlongwa, M.-S. Hosseini, A.K. Hsiao, I. Iavicoli, S.E. Ibitoye, I.M. Ilic, M.D. Ilic, S.M.S. Islam, M.D. Janodia, R.P. Jha, H.A. Jindal, J.B. Jonas, G.G. Kabito, H. Kandel, R.J. Kaur, V.R. Keshri, Y.S. Khader, E.A. Khan, M.J. Khan, M.A. Khan, H.R. Khayat Kashani, J. Khubchandani, Y.J. Kim, A. Kisa, J. Klugarová, A.-A. Kolahi, H.R. Koohestani, A. Koyanagi, G.A. Kumar, N. Kumar, T. Lallukka, S. Lasrado, W.-C. Lee, Y.H. Lee, A. Mahmoodpoor, J.N. Malagón-Rojas, M.-R. Malekpour, R. Malekzadeh, N. Malih, M.M. Mehndiratta, E. Mehrabi Nasab, R.G. Menezes, A.-F.A. Mentis, M.K. Mesregah, T.R. Miller, M. Mirza-Aghazadeh-Attari, M. Mobarakabadi, Y. Mohammad, E. Mohammadi, S. Mohammed, A.H. Mokdad, S. Momtazmanesh, L. Monasta, M.A. Moni, E. Mostafavi, C.J.L. Murray, T.S. Nair, J. Nazari, S.A. Nejadghaderi, S. Neupane, S. Neupane Kandel, C.T. Nguyen, A. Nowroozi, H. Okati-Aliabad, E. Omer, A. Oulhaj, M.O. Owolabi, S. Panda-Jonas, A. Pandey, E.-K. Park, S. Pawar, P. Pedersini, J. Pereira, M.F.P. Peres, I.-R. Petcu, M. Pourahmadi, A. Radfar, S. Rahimi-Dehgolan, V. Rahimi-Movaghar, M. Rahman, A.M. Rahmani, N. Rajai, C.R. Rao, V. Rashedi, M.-M. Rashidi, Z.A. Ratan, D.L. Rawaf, S. Rawaf, A.M.N. Renzaho, N. Rezaei, Z. Rezaei, L. Roever, G.de A. Ruela, B. Saddik, A. Sahebkar, S. Salehi, F. Sanmarchi, S.G. Sepanlou, S. Shahabi, S. Shahrokhi, E. Shaker, M. Shamsi, M. Shannawaz, S. Sharma, M. Shaygan, R.A. Sheikhi, J.K. Shetty, R. Shiri, S. Shivalli, P. Shobeiri, M.M. Sibhat,

A. Singh, J.A. Singh, H. Slater, M. Solmi, R. Somayaji, K.-K. Tan, R. Thapar, S.A. Tohidast, S. Valadan Tahbaz, R. Valizadeh, T.J. Vasankari, N. Venketasubramanian, V. Vlassov, B. Vo, Y.-P. Wang, T. Wiangkham, L. Yadav, A. Yadollahpour, S.H. Yahyazadeh Jabbari, L. Yang, F. Yazdanpanah, N. Yonemoto, M.Z. Younis, I. Zare, A. Zarrintan, M. Zoladl, T. Vos, L.M. March, Global, regional, and national burden of low back pain, 1990–2020, its attributable risk factors, and projections to 2050: a systematic analysis of the Global Burden of Disease Study 2021, Lancet Rheumatol. 5 (2023) e316–e329, doi:10.1016/S2665-9913(23)00098-X.

[2] L. Soares Fonseca, J. Pereira Silva, M. Bastos Souza, M. Gabrich Moraes Campos, R. de Oliveira Mascarenhas, H. de Jesus Silva, L. Souza Máximo Pereira, M. Xavier Oliveira, V. Cunha Oliveira, Effectiveness of pharmacological and non-pharmacological therapy on pain intensity and disability in older people with chronic nonspecific low back pain: a systematic review with meta-analysis, Eur. Spine J. (2023), doi:10.1007/s00586-023-07857-4.

[3] K. Luoma, H. Riihimäki, R. Luukkonen, R. Raininko, E. Viikari-Juntura, A. Lamminen, Low back pain in relation to lumbar disc degeneration, Spine (Phila. Pa. 1976) 25 (2000) 487–492, doi:10.1097/00007632-200002150-00016.

[4] W. Brinjikji, F.E. Diehn, J.G. Jarvik, C.M. Carr, D.F. Kallmes, M.H. Murad, P.H. Luetmer, MRI findings of disc degeneration are more prevalent in adults with low back pain than in asymptomatic controls: a systematic review and meta-analysis, Am. J. Neuroradiol. 36 (2015) 2394–2399, doi:10.3174/ajnr.A4498.

[5] P. Bermudez-Lekerika, K.B. Crump, S. Tseranidou, A. Nüesch, E. Kanelis, A. Alminnawi, L. Baumgartner, E. Muñoz-Moya, R. Compte, F. Gualdi, L.G. Alexopoulos, L. Geris, K. Wuertz-Kozak, C.L. Le Maitre, J. Noailly, B. Gantenbein, Immuno-modulatory effects of intervertebral disc cells, Front. Cell Dev. Biol. (2022) 10, doi:10.3389/fcell.2022.924692.

[6] C.L. Le Maitre, A.J. Freemont, J.A. Hoyland, Localization of degradative enzymes and their inhibitors in the degenerate human intervertebral disc, J. Pathol. (2004) 204, doi:10.1002/path.1608.

[7] L. Baumgartner, K. Wuertz-Kozak, C.L. Le Maitre, F. Wignall, S.M. Richardson, J. Hoyland, C.R. Wills, M.A. González Ballester, M. Neidlin, L.G. Alexopoulos, J. Noailly, Multiscale regulation of the intervertebral disc: achievements in experimental, in silico, and regenerative research, Int. J. Mol. Sci. (2021) 22, doi:10.3390/ijms22020703.

[8] S. Roberts, B. Caterson, J. Menage, E.H. Evans, D.C. Jaffray, S.M. Eisenstein, Matrix metalloproteinases and aggrecanase, Spine (Phila. Pa. 1976) 25 (2000) 3005–3013, doi:10.1097/00007632-200012010-00007.

[9] C.L. Le Maitre, A. Pockert, D.J. Buttle, A.J. Freemont, J.A. Hoyland, Matrix synthesis and degradation in human intervertebral disc degeneration, Biochem. Soc. Trans. (2007) 35, doi:10.1042/BST0350652.

[10] J.P. Urban, J.F. McMullin, Swelling pressure of the inervertebral disc: influence of proteoglycan and collagen contents, Biorheology 22 (1985) 145–157, doi:10.3233/bir-1985-22205.

[11] J.P.G. Urban, J.F. McMullin, Swelling pressure of the lumbar intervertebral discs, in: Spine (Phila. Pa. 1976), 13, 1988, pp. 179–187, doi:10.1097/00007632-198802000-00009.

[12] J.P.G. Urban, A. Maroudas, The measurement of fixed charged density in the intervertebral disc, Biochim. Biophys. Acta - Gen. Subj. 586 (1979) 166–178, doi:10.1016/0304-4165(79)90415-X.

[13] E. Salzer, V.H.M. Mouser, M.A. Tryfonidou, K. Ito, A bovine nucleus pulposus explant culture model, J. Orthop. Res. 40 (2022) 2089–2102, doi:10.1002/jor.25226.

[14] C. Neidlinger-Wilke, F. Galbusera, H. Pratsinis, E. Mavrogonatou, A. Mietsch, D. Kletsas, H.-J. Wilke, Mechanical loading of the intervertebral disc: from the macroscopic to the cellular level, Eur. Spine J. 23 (2014) 333–343, doi:10.1007/s00586-013-2855-9.

[15] M.A. Adams, P. Dolan, Intervertebral disc degeneration: evidence for two distinct phenotypes, J. Anat. 221 (2012) 497–506, doi:10.1111/j.1469-7580.2012.01551.x.

[16] M.A. Adams, P.J. Roughley, What is intervertebral disc degeneration, and what causes it? Spine (Phila. Pa. 1976) 31 (2006) 2151–2161, doi:10.1097/01.brs.0000231761.73859.2c.

[17] J.P.G. Urban, The role of the physicochemical environment in determining disc cell behaviour, Biochem. Soc. Trans. 30 (2002) 858–863, doi:10.1042/bst0300858.

[18] S. Sivan, C. Neidlinger-Wilke, K. Würtz, A. Maroudas, J.P.G. Urban, Diurnal fluid expression and activity of intervertebral disc cells, Biorheology 43 (2006) 283–291.

[19] S.J. Ferguson, K. Ito, L.-P. Nolte, Fluid flow and convective transport of solutes within the intervertebral disc, J. Biomech. 37 (2004) 213–221, doi:10.1016/S0021-9290(03)00250-1.

[20] W. Johannessen, E.J. Vresilovic, A.C. Wright, D.M. Elliott, Intervertebral disc mechanics are restored following cyclic loading and unloaded recovery, Ann. Biomed. Eng. 32 (2004) 70–76, doi:10.1023/B:ABME.0000007792.19071.8c.

[21] K.S. Emanuel, A.J. van der Veen, C.M.E. Rustenburg, T.H. Smit, I. Kingma, Osmosis and viscoelasticity both contribute to time-dependent behaviour of the intervertebral disc under compressive load: a caprine in vitro study, J. Biomech. 70 (2018) 10–15, doi:10.1016/j.jbiomech.2017.10.010.

[22] P.-P.A. Vergroesen, A.J. van der Veen, K.S. Emanuel, J.H. van Dieën, T.H. Smit, The poro-elastic behaviour of the intervertebral disc: a new perspective on diurnal fluid flow, J. Biomech. 49 (2016) 857–863, doi:10.1016/j.jbiomech.2015.11.041.

[23] M. Adams, P. Dolan, W. Hutton, R. Porter, Diurnal changes in spinal mechanics and their clinical significance, J. Bone Joint Surg. Br. 72-B (1990) 266–270, doi:10.1302/0301-620X.72B2.2138156.

[24] C. Le Maitre, A.J. Freemont, J. Hoyland, The role of interleukin-1 in the pathogenesis of human Intervertebral disc degeneration, Arthritis Res. Ther. 7 (2005) R732, doi:10.1186/ar1732.

[25] K.L.E. Phillips, K. Cullen, N. Chiverton, A.L.R. Michael, A.A. Cole, L.M. Breakwell, G. Haddock, R.A.D. Bunning, A.K. Cross, C.L. Le Maitre, Potential roles of cytokines and chemokines in human intervertebral disc degeneration: interleukin-1 is a master regulator of catabolic processes, Osteoarthr. Cartil. 23 (2015), doi:10.1016/j.joca.2015.02.017.

[26] K.L.E. Phillips, N. Chiverton, A.L.R. Michael, A.A. Cole, L.M. Breakwell, G. Haddock, R.A.D. Bunning, A.K. Cross, C.L. Le Maitre, The cytokine and chemokine expression profile of nucleus pulposus cells: implications for degeneration and regeneration of the intervertebral disc, Arthritis Res. Ther. 15 (2013), doi:10.1186/ar4408.

[27] J. Wang, Y. Tian, K.L.E. Phillips, N. Chiverton, G. Haddock, R.A. Bunning, A.K. Cross, I.M. Shapiro, C.L. Le Maitre, M.V. Risbud, Tumor necrosis factor α- And interleukin-1β-dependent induction of CCL3 expression by nucleus pulposus cells promotes macrophage migration through CCR1, Arthritis Rheum 65 (2013), doi:10.1002/art.37819.

[28] A.L.A Binch, A.A. Cole, L.M. Breakwell, A.L.R. Michael, N. Chiverton, A.K. Cross, C.L. Le Maitre, Expression and regulation of neurotrophic and angiogenic factors during human intervertebral disc degeneration, Arthritis Res. Ther. (2014) 16, doi:10.1186/s13075-014-0416-1.

[29] W.E.B. Johnson, B. Caterson, S.M. Eisenstein, D.L. Hynds, D.M. Snow, S. Roberts, Human intervertebral disc aggrecan inhibits nerve growth in vitro, Arthritis Rheum 46 (2002) 2658–2664, doi:10.1002/art.10585.

[30] C.C.M. Chan, C.R. Roberts, J.D. Steeves, W. Tetzlaff, Aggrecan components differentially modulate nerve growth factor–responsive and neurotrophin-3-responsive dorsal root ganglion neurite growth, J. Neurosci. Res. 86 (2008) 581–592, doi:10.1002/jnr.21522.

[31] S.K. Tolofari, S.M. Richardson, A.J. Freemont, J.A. Hoyland, Expression of semaphorin 3A and its receptors in the human intervertebral disc: potential role in regulating neural ingrowth in the degenerate intervertebral disc, Arthritis Res. Ther. 12 (2010) R1, doi:10.1186/ar2898.

[32] A.L.A. Binch, A.A. Cole, L.M. Breakwell, A.L.R. Michael, N. Chiverton, L.B. Creemers, A.K. Cross, C.L. Le Maitre, Class 3 semaphorins expression and association with innervation and angiogenesis within the degenerate human intervertebral disc, Oncotarget 6 (2015), doi:10.18632/oncotarget.4274.

[33] A.J. Freemont, A. Watkins, C. Le Maitre, P. Baird, M. Jeziorska, M.T.N. Knight, E.R.S. Ross, J.P. O'Brien, J.A. Hoyland, Nerve growth factor expression and innervation of the painful intervertebral disc, J. Pathol. 197 (2002), doi:10.1002/path.1108.

[34] D. Purmessur, A.J. Freemont, J.A. Hoyland, Expression and regulation of neurotrophins in the nondegenerate and degenerate human intervertebral disc, Arthritis Res. Ther. 10 (2008) R99, doi:10.1186/ar2487.

[35] A.L.A. Binch, A.A. Cole, L.M. Breakwell, A.L.R. Michael, N. Chiverton, L.B. Creemers, A.K. Cross, C.L. Le Maitre, Nerves are more abundant than blood vessels in the degenerate human intervertebral disc, Arthritis Res. Ther. (2015) 17, doi:10.1186/s13075-015-0889-6.

[36] P. Lama, C.L. Le Maitre, I.J. Harding, P. Dolan, M.A. Adams, Nerves and blood vessels in degenerated intervertebral discs are confined to physically disrupted tissue, J. Anat. (2018) 233, doi:10.1111/joa.12817.

[37] A. Freemont, T. Peacock, P. Goupille, J. Hoyland, J. O'Brien, M. Jayson, Nerve ingrowth into diseased intervertebral disc in chronic back pain, Lancet 350 (1997) 178–181, doi:10.1016/S0140-6736(97)02135-1.

[38] P. Lama, C.L. Le Maitre, P. Dolan, J.F. Tarlton, I.J. Harding, M.A. Adams, Do intervertebral discs degenerate before they herniate, or after? Bone Jt. J. 95 B (2013), doi:10.1302/0301-620X.95B8.31660.

[39] P.-P.A. Vergroesen, I. Kingma, K.S. Emanuel, R.J.W. Hoogendoorn, T.J. Welting, B.J. van Royen, J.H. van Dieën, T.H. Smit, Mechanics and biology in intervertebral disc degeneration: a vicious circle, Osteoarthr. Cartil. 23 (2015) 1057–1070, doi:10.1016/j.joca.2015.03.028.

[40] T. Lindsey, A.M. Dydyk, Spinal osteoarthritis, 2023.

[41] N. Fine, S. Lively, C.A. Séguin, A.V. Perruccio, M. Kapoor, R. Rampersaud, Intervertebral disc degeneration and osteoarthritis: a common molecular disease spectrum, Nat. Rev. Rheumatol. 19 (2023) 136–152, doi:10.1038/s41584-022-00888-z.

[42] A. Zhang, Z. Cheng, Y. Chen, P. Shi, W. Gan, Y. Zhang, Emerging tissue engineering strategies for annulus fibrosus therapy, Acta Biomater. 167 (2023) 1–15, doi:10.1016/j.actbio.2023.06.012.

[43] J. Zhang, W. Zhang, T. Sun, J. Wang, Y. Li, J. Liu, Z. Li, The influence of intervertebral disc microenvironment on the biological behavior of engrafted mesenchymal stem cells, Stem Cells Int. 2022 (2022) 1–24, doi:10.1155/2022/8671482.

[44] I.L. Mohd Isa, S.A. Mokhtar, S.A. Abbah, M.B. Fauzi, A. Devitt, A. Pandit, Intervertebral disc degeneration: biomaterials and tissue engineering strategies toward precision medicine, Adv. Healthc. Mater. (2022) 11, doi:10.1002/adhm.202102530.

[45] L.J. Smith, L. Silverman, D. Sakai, C.L. Le Maitre, R.L. Mauck, N.R. Malhotra, J.C. Lotz, C.T. Buckley, Advancing cell therapies for intervertebral disc regeneration from the lab to the clinic: recommendations of the ORS spine section, JOR Spine 1 (2018), doi:10.1002/jsp2.1036.

[46] J. Schol, D. Sakai, Cell therapy for intervertebral disc herniation and degenerative disc disease: clinical trials, Int. Orthop. 43 (2019) 1011–1025, doi:10.1007/s00264-018-4223-1.

[47] D. Sakai, J. Schol, M. Watanabe, Clinical development of regenerative medicine targeted for intervertebral disc disease, Medicina (B. Aires) 58 (2022) 267, doi:10.3390/medicina58020267.
[48] M. Loibl, K. Wuertz-Kozak, G. Vadala, S. Lang, J. Fairbank, J.P. Urban, Controversies in regenerative medicine: should intervertebral disc degeneration be treated with mesenchymal stem cells? JOR Spine 2 (2019), doi:10.1002/jsp2.1043.
[49] R.J. Williams, M.A. Tryfonidou, J.W. Snuggs, C.L. Le Maitre, Cell sources proposed for nucleus pulposus regeneration, JOR Spine 4 (2021), doi:10.1002/jsp2.1175.
[50] Z.L. Li, Q. Lu, J.R. Honiball, S.H. Wan, K.W. Yeung, K.M. Cheung, Mechanical characterization and design of biomaterials for nucleus pulposus replacement and regeneration, J. Biomed. Mater. Res. Part A. (2023), doi:10.1002/jbm.a.37593.
[51] H.-J. Wilke, F. Heuer, C. Neidlinger-Wilke, L. Claes, Is a collagen scaffold for a tissue engineered nucleus replacement capable of restoring disc height and stability in an animal model? Eur. Spine J. 15 (2006) 433–438, doi:10.1007/s00586-006-0177-x.
[52] E. Durdag, O. Ayden, S. Albayrak, I.B. Atci, E. Armagan, Fragmentation to epidural space: first documented complication of Gelstix(TM.), Turk. Neurosurg. 24 (2014) 602–605, doi:10.5137/1019-5149.JTN.9328-13.1.
[53] D.H. Kim, J.T. Martin, S.E. Gullbrand, D.M. Elliott, L.J. Smith, H.E. Smith, R.L. Mauck, Fabrication, maturation, and implantation of composite tissue-engineered total discs formed from native and mesenchymal stem cell combinations, Acta Biomater 114 (2020) 53–62, doi:10.1016/j.actbio.2020.05.039.
[54] S.A. Rundell, H.L. Guerin, J.D. Auerbach, S.M. Kurtz, Effect of nucleus replacement device properties on lumbar spine mechanics, Spine (Phila. Pa. 1976) 34 (2009) 2022–2032, doi:10.1097/BRS.0b013e3181af1d5a.
[55] A. Joshi, C.J. Massey, A. Karduna, E. Vresilovic, M. Marcolongo, The effect of nucleus implant parameters on the compressive mechanics of the lumbar intervertebral disc: a finite element study, J. Biomed. Mater. Res. Part B Appl. Biomater. 90B (2009) 596–607, doi:10.1002/jbm.b.31322.
[56] C. Zhang, S.E. Gullbrand, T.P. Schaer, S. Boorman, D.M. Elliott, W. Chen, G.R. Dodge, R.L. Mauck, N.R. Malhotra, L.J. Smith, Combined hydrogel and mesenchymal stem cell therapy for moderate-severity disc degeneration in goats, Tissue Eng. Part A. 27 (2021) 117–128, doi:10.1089/ten.tea.2020.0103.
[57] K. Yang, Z. Song, D. Jia, J. Ma, Y. Huo, Y. Zhao, W. Zhang, W. Ding, Z. Wu, S. Yang, Comparisons between needle puncture and chondroitinase ABC to induce intervertebral disc degeneration in rabbits, Eur. Spine J. 31 (2022) 2788–2800, doi:10.1007/s00586-022-07287-8.
[58] F. Romaniyanto, F. Mahyudin, D.N. Utomo, H. Suroto, W.A. Sari, M.S. Fachreza, D. Sadewa, D.N. Dzikri, F. Nofaldi, Effectivity of puncture method for intervertebral disc degeneration animal models: review article, Ann. Med. Surg. 85 (2023) 3501–3505, doi:10.1097/MS9.0000000000000829.
[59] M. Alini, S.M. Eisenstein, K. Ito, C. Little, A.A. Kettler, K. Masuda, J. Melrose, J. Ralphs, I. Stokes, H.J. Wilke, Are animal models useful for studying human disc disorders/degeneration? Eur. Spine J. 17 (2008) 2–19, doi:10.1007/s00586-007-0414-y.
[60] V.L. Boyes, R. Janani, S. Partridge, L.A. Fielding, C. Breen, J. Foulkes, C.L. Le Maitre, C. Sammon, One-pot precipitation polymerisation strategy for tuneable injectable Laponite®-pNIPAM hydrogels: polymerisation, processability and beyond, Polymer (Guildf) (2021) 233, doi:10.1016/j.polymer.2021.124201.
[61] A.A. Thorpe, V.L. Boyes, C. Sammon, C.L. Le Maitre, Thermally triggered injectable hydrogel, which induces mesenchymal stem cell differentiation to nucleus pulposus cells: potential for regeneration of the intervertebral disc, Acta Biomater 36 (2016), doi:10.1016/j.actbio.2016.03.029.
[62] A.A. Thorpe, G. Dougill, L. Vickers, N.D. Reeves, C. Sammon, G. Cooper, C.L. Le Maitre, Thermally triggered hydrogel injection into bovine intervertebral disc tissue explants induces differentiation of mesenchymal stem cells and restores mechanical function, Acta Biomater. 54 (2017), doi:10.1016/j.actbio.2017.03.010.
[63] J.W. Snuggs, K.S. Emanuel, C. Rustenburg, R. Janani, S. Partridge, C. Sammon, T.H. Smit, C.L. Le Maitre, Injectable biomaterial induces regeneration of the intervertebral disc in a caprine loaded disc culture model, Biomater. Sci. (2023) 11, doi:10.1039/d3bm00150d.
[64] E. Salzer, T.C. Schmitz, V.H.M. Mouser, A. Vernengo, B. Gantenbein, J.U. Jansen, C. Neidlinger-Wilke, H.-J. Wilke, S. Grad, C.L. Le Maitre, M.A. Tryfonidou, K. Ito, Ex vivo intervertebral disc cultures: degeneration-induction methods and their implications for clinical translation, Eur. Cells Mater. 45 (2023), doi:10.22203/eCM.v045a07.
[65] C.L. Le Maitre, J.A. Hoyland, A.J. Freemont, Studies of human intervertebral disc cell function in a constrained in vitro tissue culture system, in: Spine (Phila. Pa. 1976), 2004, p. 29, doi:10.1097/00007632-200406010-00006.
[66] S.N. Tang, A.F. Bonilla, N.O. Chahine, A.C. Colbath, J.T. Easley, S. Grad, L. Haglund, C.L. Le Maitre, V. Leung, A.M. McCoy, D. Purmessur, S.Y. Tang, S. Zeiter, L.J. Smith, Controversies in spine research: organ culture versus in vivo models for studies of the intervertebral disc, JOR Spine 5 (2022), doi:10.1002/jsp2.1235.
[67] R. Gawri, F. Mwale, J. Ouellet, P.J. Roughley, T. Steffen, J. Antoniou, L. Haglund, Development of an organ culture system for long-term survival of the intact human intervertebral disc, Spine (Phila. Pa. 1976) 36 (2011) 1835–1842, doi:10.1097/BRS.0b013e3181f81314.
[68] H. Cherif, D.G. Bisson, M. Mannarino, O. Rabau, J.A. Ouellet, L. Haglund, Senotherapeutic drugs for human intervertebral disc degeneration and low back pain, Elife (2020) 9, doi:10.7554/eLife.54693.
[69] D. Rosenzweig, R. Gawri, J. Moir, L. Beckman, D. Eglin, T. Steffen, P. Roughley, J.A. Ouellet, L. Haglund, Dynamic loading, matrix maintenance and cell injection therapy of human intervertebral discs cultured in a bioreactor, Eur. Cells Mater. 31 (2016) 26–39, doi:10.22203/eCM.v031a03.
[70] B.A. Walter, S. Illien-Jünger, P.R. Nasser, A.C. Hecht, J.C. Iatridis, Development and validation of a bioreactor system for dynamic loading and mechanical characterization of whole human intervertebral discs in organ culture, J. Biomech. 47 (2014) 2095–2101, doi:10.1016/j.jbiomech.2014.03.015.
[71] C.L. Le Maitre, C.L. Dahia, M. Giers, S. Illien-Junger, C. Cicione, D. Samartzis, G. Vadala, A. Fields, J. Lotz, Development of a standardized histopathology scoring system for human intervertebral disc degeneration: an Orthopaedic Research Society Spine Section Initiative, JOR Spine 4 (2021), doi:10.1002/jsp2.1167.
[72] H.-J. Wilke, F. Rohlmann, C. Neidlinger-Wilke, K. Werner, L. Claes, A. Kettler, Validity and interobserver agreement of a new radiographic grading system for intervertebral disc degeneration: part I. Lumbar spine, Eur. Spine J 15 (2006) 720–730, doi:10.1007/s00586-005-1029-9.
[73] S.B. Tibrewal, M.J. Pearcy, Lumbar intervertebral disc heights in normal subjects and patients with disc herniation, Spine (Phila. Pa. 1976) 10 (1985) 452–454, doi:10.1097/00007632-198506000-00009.
[74] H. Cherif, D. Bisson, P. Jarzem, M. Weber, J. Ouellet, L. Haglund, Curcumin and o-vanillin exhibit evidence of senolytic activity in human IVD cells in vitro, J. Clin. Med. 8 (2019) 433, doi:10.3390/jcm8040433.
[75] B. PAGE, M. PAGE, C. NOEL, A new fluorometric assay for cytotoxicity measurements in-vitro, Int. J. Oncol. (1993), doi:10.3892/ijo.3.3.473.
[76] K. Fujii, A. Lai, N. Korda, W.W. Hom, T.W. Evashwick-Rogler, P. Nasser, A.C. Hecht, J.C. Iatridis, Ex-vivo biomechanics of repaired rat intervertebral discs using genipin crosslinked fibrin adhesive hydrogel, J. Biomech. 113 (2020) 110100, doi:10.1016/j.jbiomech.2020.110100.
[77] X. Li, Y. Liu, L. Li, R. Huo, F. Ghezelbash, Z. Ma, G. Bao, S. Liu, Z. Yang, M.H. Weber, N.Y.K. Li-Jessen, L. Haglund, J. Li, Tissue-mimetic hybrid bioadhesives for intervertebral disc repair, Mater. Horizons. 10 (2023) 1705–1718, doi:10.1039/D2MH01242A.
[78] H. Yang, M.G. Jekir, M.W. Davis, T.M. Keaveny, Effective modulus of the human intervertebral disc and its effect on vertebral bone stress, J. Biomech. 49 (2016) 1134–1140, doi:10.1016/j.jbiomech.2016.02.045.
[79] J.P. Thompson, R.H. Pearce, M.T. Schechter, M.E. Adams, I.K.Y. Tsang, P.B. Bishop, Preliminary evaluation of a scheme for grading the gross morphology of the human intervertebral disc, in: Spine (Phila. Pa. 1976), 15, 1990, pp. 411–415, doi:10.1097/00007632-199005000-00012.
[80] A. Binch, J. Snuggs, C.L. Le Maitre, Immunohistochemical analysis of protein expression in formalin fixed paraffin embedded human intervertebral disc tissues, JOR Spine 3 (2020), doi:10.1002/jsp2.1098.
[81] J.-J. Pfannkuche, W. Guo, S. Cui, J. Ma, G. Lang, M. Peroglio, R.G. Richards, M. Alini, S. Grad, Z. Li, Intervertebral disc organ culture for the investigation of disc pathology and regeneration – benefits, limitations, and future directions of bioreactors, Connect. Tissue Res. 61 (2020) 304–321, doi:10.1080/03008207.2019.1665652.
[82] P. Li, M. Zhang, Z. Chen, B. Tian, X. Kang, Tissue-engineered injectable gelatin–methacryloyl hydrogel-based adjunctive therapy for intervertebral disc degeneration, ACS Omega 8 (2023) 13509–13518, doi:10.1021/acsomega.3c00211.
[83] J. Luo, A. Darai, T. Pongkulapa, B. Conley, L. Yang, I. Han, K.-B. Lee, Injectable bioorthogonal hydrogel (BIOGEL) accelerates tissue regeneration in degenerated intervertebral discs, Bioact. Mater. 23 (2023) 551–562, doi:10.1016/j.bioactmat.2022.11.017.
[84] R.M. Jarrah, M.D.A. Potes, X. Vitija, S. Durrani, A.K. Ghaith, W. Mualem, C. Zamanian, A.R. Bhandarkar, M. Bydon, Alginate hydrogels: a potential tissue engineering intervention for intervertebral disc degeneration, J. Clin. Neurosci. 113 (2023) 32–37, doi:10.1016/j.jocn.2023.05.001.
[85] W. Li, P. Zhou, B. Yan, M. Qi, Y. Chen, L. Shang, J. Guan, L. Zhang, Y. Mao, Disc regeneration by injectable fucoidan-methacrylated dextran hydrogels through mechanical transduction and macrophage immunomodulation, J. Tissue Eng. 14 (2023), doi:10.1177/20417314231180050.
[86] U. Berlemann, O. Schwarzenbach, An injectable nucleus replacement as an adjunct to microdiscectomy: 2 year follow-up in a pilot clinical study, Eur. Spine J. 18 (2009) 1706–1712, doi:10.1007/s00586-009-1136-0.
[87] S.E. Gullbrand, N.R. Malhotra, T.P. Schaer, Z. Zawacki, J.T. Martin, J.R. Bendigo, A.H. Milby, G.R. Dodge, E.J. Vresilovic, D.M. Elliott, R.L. Mauck, L.J. Smith, A large animal model that recapitulates the spectrum of human intervertebral disc degeneration, Osteoarthr. Cartil. 25 (2017) 146–156, doi:10.1016/j.joca.2016.08.006.
[88] N. Willems, G. Mihov, G.C.M. Grinwis, M. van Dijk, D. Schumann, C. Bos, G.J. Strijkers, W.J.A. Dhert, B.P. Meij, L.B. Creemers, M.A. Tryfonidou, Safety of intradiscal injection and biocompatibility of polyester amide microspheres in a canine model predisposed to intervertebral disc degeneration, J. Biomed. Mater. Res. Part B Appl. Biomater. 105 (2017) 707–714, doi:10.1002/jbm.b.33579.
[89] G. Lang, Y. Liu, J. Geries, Z. Zhou, D. Kubosch, N. Südkamp, R.G. Richards, M. Alini, S. Grad, Z. Li, An intervertebral disc whole organ culture system to investigate proinflammatory and degenerative disc disease condition, J. Tissue Eng. Regen. Med. 12 (2018) e2051–e2061, doi:10.1002/term.2636.
[90] K. Latka, K. Kozlowska, M. Waligora, W. Kolodziej, T. Olbrycht, J. Chowaniec, S. Hendryk, M. Latka, D. Latka, Efficacy of DiscoGel in treatment of degenerative disc disease: a prospective 1-year observation of 67 patients, Brain Sci 11 (2021) 1434, doi:10.3390/brainsci11111434.
[91] P.J. Roughley, J.S. Mort, The role of aggrecan in normal and osteoarthritic cartilage, J. Exp. Orthop. 1 (2014) 8, doi:10.1186/s40634-014-0008-7.

[92] D.S. Perie, J.J. Maclean, J.P. Owen, J.C. Iatridis, Correlating material properties with tissue composition in enzymatically digested bovine annulus fibrosus and nucleus pulposus tissue, Ann. Biomed. Eng. 34 (2006) 769–777, doi:10.1007/s10439-006-9091-y.
[93] W. Koeller, S. Muehlhaus, W. Meier, F. Hartmann, Biomechanical properties of human intervertebral discs subjected to axial dynamic compression—influence of age and degeneration, J. Biomech. 19 (1986) 807–816, doi:10.1016/0021-9290(86)90131-4.
[94] B.L. Showalter, N.R. Malhotra, E.J. Vresilovic, D.M. Elliott, Nucleotomy reduces the effects of cyclic compressive loading with unloaded recovery on human intervertebral discs, J. Biomech. 47 (2014) 2633–2640, doi:10.1016/j.jbiomech.2014.05.018.
[95] B.L. Showalter, D.M. Elliott, W. Chen, N.R. Malhotra, Evaluation of an in situ gelable and injectable hydrogel treatment to preserve human disc mechanical function undergoing physiologic cyclic loading followed by hydrated recovery, J. Biomech. Eng. (2015) 137, doi:10.1115/1.4030530.
[96] J. Mochida, K. Nishimura, T. Nomura, E. Toh, M. Chiba, The importance of preserving disc structure in surgical approaches to lumbar disc herniation, Spine (Phila. Pa. 1976) 21 (1996) 1556–1563, doi:10.1097/00007632-199607010-00014.
[97] Y. Lu, M.J. Sherratt, M.-C. Wang, C. Baldock, Tissue specific differences in fibrillin microfibrils analysed using single particle image analysis, J. Struct. Biol. 155 (2006) 285–293, doi:10.1016/j.jsb.2006.03.021.
[98] M.A. Cattell, J.C. Anderson, P.S. Hasleton, Age-related changes in amounts and concentrations of collagen and elastin in normotensive human thoracic aorta, Clin. Chim. Acta. 245 (1996) 73–84, doi:10.1016/0009-8981(95)06174-6.
[99] G.D. O'Connell, N.R. Malhotra, E.J. Vresilovic, D.M. Elliott, The effect of nucleotomy and the dependence of degeneration of human intervertebral disc strain in axial compression, Spine (Phila. Pa. 1976) 36 (2011) 1765–1771, doi:10.1097/BRS.0b013e318216752f.
[100] G.D. O'Connell, N.T. Jacobs, S. Sen, E.J. Vresilovic, D.M. Elliott, Axial creep loading and unloaded recovery of the human intervertebral disc and the effect of degeneration, J. Mech. Behav. Biomed. Mater. 4 (2011) 933–942, doi:10.1016/j.jmbbm.2011.02.002.
[101] A.J. Michalek, J.C. Iatridis, Height and torsional stiffness are most sensitive to annular injury in large animal intervertebral discs, Spine J. 12 (2012) 425–432, doi:10.1016/j.spinee.2012.04.001.
[102] J.C. Iatridis, L.A. Setton, M. Weidenbaum, V.C. Mow, Alterations in the mechanical behavior of the human lumbar nucleus pulposus with degeneration and aging, J. Orthop. Res. 15 (1997) 318–322, doi:10.1002/jor.1100150224.
[103] K.K. Cheng, S.H. Berven, S.S. Hu, J.C. Lotz, Intervertebral discs from spinal nondeformity and deformity patients have different mechanical and matrix properties, Spine J 14 (2014) 522–530, doi:10.1016/j.spinee.2013.06.089.
[104] L.A. Setton, J. Chen, Mechanobiology of the Intervertebral Disc and Relevance to Disc Degeneration, J. Bone Jt. Surg. 88 (2006) 52–57, doi:10.2106/JBJS.F.00001.
[105] M.G. Muriuki, R.M. Havey, L.I. Voronov, G. Carandang, M.R. Zindrick, M.A. Lorenz, L. Lomasney, A.G. Patwardhan, Effects of motion segment level, Pfirrmann intervertebral disc degeneration grade and gender on lumbar spine kinematics, J. Orthop. Res. 34 (2016) 1389–1398, doi:10.1002/jor.23232.
[106] NCT04727385, Intervertebral DXM gel injection in adults with painful lumbar degenerative disc disease (DXM gel), (n.d.). https://clinicaltrials.gov/study/NCT04727385 (accessed September 21, 2023).
[107] B. Gantenbein, S. Illien-Jünger, S. Chan, J. Walser, L. Haglund, S. Ferguson, J. Iatridis, S. Grad, Organ culture bioreactors – platforms to study human intervertebral disc degeneration and regenerative therapy, Curr. Stem Cell Res. Ther. 10 (2015) 339–352, doi:10.2174/1574888x10666150312102948.
[108] D. Rosenzweig, R. Fairag, A. Mathieu, L. Li, D. Eglin, M. D'Este, T. Steffen, M. Weber, J. Ouellet, L. Haglund, Thermoreversible hyaluronan-hydrogel and autologous nucleus pulposus cell delivery regenerates human intervertebral discs in an ex vivo, physiological organ culture model, Eur. Cells Mater. 36 (2018) 200–217, doi:10.22203/eCM.v036a15.
[109] F. Mwale, H.T. Wang, P. Roughley, J. Antoniou, L. Haglund, Link N and mesenchymal stem cells can induce regeneration of the early degenerate intervertebral disc, Tissue Eng. Part A. 20 (2014) 2942–2949, doi:10.1089/ten.tea.2013.0749.
[110] F. Russo, L. Ambrosio, M. Peroglio, W. Guo, S. Wangler, J. Gewiess, S. Grad, M. Alini, R. Papalia, G. Vadalà, V. Denaro, A hyaluronan and platelet-rich plasma hydrogel for mesenchymal stem cell delivery in the intervertebral disc: an organ culture study, Int. J. Mol. Sci. 22 (2021) 2963, doi:10.3390/ijms22062963.
[111] M. Peroglio, D. Eglin, L.M. Benneker, M. Alini, S. Grad, Thermoreversible hyaluronan-based hydrogel supports in vitro and ex vivo disc-like differentiation of human mesenchymal stem cells, Spine J. 13 (2013) 1627–1639, doi:10.1016/j.spinee.2013.05.029.
[112] M. Loepfe, A. Duss, K.-A. Zafeiropoulou, O. Björgvinsdóttir, M. D'Este, D. Eglin, G. Fortunato, J. Klasen, S.J. Ferguson, K. Wuertz-Kozak, O. Krupkova, Electrospray-based microencapsulation of epigallocatechin 3-gallate for local delivery into the intervertebral disc, Pharmaceutics 11 (2019) 435, doi:10.3390/pharmaceutics11090435.
[113] F. Han, Z. Tu, Z. Zhu, D. Liu, Q. Meng, Q. Yu, Y. Wang, J. Chen, T. Liu, F. Han, B. Li, Targeting endogenous reactive oxygen species removal and regulating regenerative microenvironment at annulus fibrosus defects promote tissue repair, ACS Nano 17 (2023) 7645–7661, doi:10.1021/acsnano.3c00093.
[114] I.L.M. Isa, A. Srivastava, D. Tiernan, P. Owens, P. Rooney, P. Dockery, A. Pandit, Hyaluronic acid based hydrogels attenuate inflammatory receptors and neurotrophins in interleukin-1β induced inflammation model of nucleus pulposus cells, Biomacromolecules 16 (2015) 1714–1725, doi:10.1021/acs.biomac.5b00168.
[115] G.Q. Teixeira, C. Leite Pereira, F. Castro, J.R. Ferreira, M. Gomez-Lazaro, P. Aguiar, M.A. Barbosa, C. Neidlinger-Wilke, R.M. Goncalves, Anti-inflammatory Chitosan/Poly-γ-glutamic acid nanoparticles control inflammation while remodeling extracellular matrix in degenerated intervertebral disc, Acta Biomater 42 (2016) 168–179, doi:10.1016/j.actbio.2016.06.013.
[116] Y. Xia, H. Wang, R. Yang, Y. Hou, Y. Li, J. Zhu, C. Fu, Biomaterials delivery strategies to repair degenerated intervertebral discs by regulating the inflammatory microenvironment, Front. Immunol. (2023) 14, doi:10.3389/fimmu.2023.1051606.
[117] E. Krock, D.H. Rosenzweig, A. Chabot-Doré, P. Jarzem, M.H. Weber, J.A. Ouellet, L.S. Stone, L. Haglund, Painful, degenerating intervertebral discs up-regulate neurite sprouting and <scp>CGRP</scp>through nociceptive factors, J. Cell. Mol. Med. 18 (2014) 1213–1225, doi:10.1111/jcmm.12268.